Journal of Geochemical Exploration 190 (2018) 154–169

Contents lists available at ScienceDirect

Journal of Geochemical Exploration

journal homepage: www.elsevier.com/locate/gexplo

Pollution, source apportionment and health risk of potentially toxic elements (PTEs) and polycyclic aromatic hydrocarbons (PAHs) in urban street dust of Mashhad, the second largest city of Iran

Ali Najmeddin[a,*], Farid Moore[a,b], Behnam Keshavarzi[a,b], Zahra Sadegh[a]

[a] Department of Earth Sciences, College of Sciences, Shiraz University, Shiraz 71454, Iran
[b] Medical geology center of Shiraz University, Iran

ARTICLE INFO

Keywords:
Potentially toxic elements (PTEs)
Polycyclic aromatic hydrocarbons (PAHs)
Simple bioaccessibility extraction test (SBET)
Street dust
Health risk assessment
Mashhad city

ABSTRACT

Street dust samples from industrial, residential and heavy density traffic areas in Mashhad metropolis were collected to study the mineralogy, distribution, accumulation, health risk assessment and probable sources of potentially toxic elements (PTEs) and polycyclic aromatic hydrocarbons (PAHs). Also, the oral bioaccessibility of PTEs using a simple bioaccessibility extraction test (SBET) was investigated. X-ray diffraction analysis of dust samples showed that the mineralogy of dust is dominated by quartz (also α-quartz), calcite (also Mg-calcite), and dolomite. Calculation of geoaccumulation index indicated that the dust is much enriched in Hg, Pb, Zn, Cu, Sb and Cd. Combined multivariate statistical and geochemical methods successfully differentiated the anthropogenic PTEs from natural ones. Zn, Hg, Pb and Cu showed high bioaccessibility. Moreover, carcinogenic and non-carcinogenic effects of PTEs due to exposure to urban street dust were assessed for both children and adults. It is found that the total amount of PAHs (Σ16 PAHs) varied from 764 to 8986.7 μg/kg, with the most serious species being 4-ring PAHs. Molecular indices and ring classes indicated that the sources of PAHs were both petrogenic and pyrogenic. The incremental lifetime cancer risks of exposure to dust PAHs for children and adults living in the study area were 7×10^{-4} and 6.2×10^{-4} respectively, indicating a high potential carcinogenic risk.

1. Introduction

Urban areas are the most densely populated regions of the world as their industrial and economic activities attract residents, and cities have become the geographic focus of intense resource inputs, energy consumption and waste emissions, which may cause many environmental problems (Luo et al., 2012). As a consequence, the quality of urban environments particularly in developing countries has declined (Brown and Peake, 2006). Street dust is a valuable medium for characterizing urban environmental quality (Liu et al., 2014; Najmeddin et al., 2017). The term 'street dust' refers to the load of deposited dust on a paved surface. However, the term refers not only to dust that collects on surfaces next to a road, but also to dust that collects on other paved surfaces, such as at industrial sites (Klees et al., 2013). The contaminants associated with street dust may harm the urban environment and endanger the ecosystem's health (Schafer et al., 2009). Street dust can be a particular risk to humans due to small particle size and inherent mobility in windy weather conditions leading to the possibility of direct and indirect exposure: direct exposure from dust can occur by inhalation and ingestion while indirect exposure results from contact with exposed skin and outer clothing which in turn can be accidentally ingested (Okorie et al., 2012). Street dust often contains elevated amounts of the potentially toxic elements (PTEs) and organic contaminants such as anthropogenic polycyclic aromatic hydrocarbons (PAHs) (Zhao et al., 2016).

PTEs may accumulate in road dust through dry deposition, impaction and interception (Mohd Han et al., 2014). The accumulation of PTEs can also result from industrial discharge, the use of oil lubricants, automobile parts and corroding building-material, asphalts, road paint and concrete (Malkoc et al., 2010; Karmacharya and Shakya, 2012; Zannoni et al., 2016; Ravankhah et al., 2016). PTEs are not biodegradable and can remain in dust for long periods of time (Saeedi et al., 2012). High concentration of PTEs causes deleterious effects on various terrestrial creatures and human beings (Kumar and Kothiyal, 2011). Some investigations show that contamination by the PTEs in the street dust strongly depends on the mineral composition and the particle size of the dust (Acosta et al., 2011; Krishna and Mohan, 2013). For risk assessment purpose, it is important to determine the more labile

* Corresponding author.
E-mail address: najmeddinali@shirazu.ac.ir (A. Najmeddin).

https://doi.org/10.1016/j.gexplo.2018.03.004
Received 19 August 2016; Received in revised form 24 February 2018; Accepted 8 March 2018
Available online 09 March 2018
0375-6742/

components, i.e., the bioaccessible fraction, in the physiological fluids (Adamson et al., 2000). Therefore, the physiologically based extraction test (PBET) and the simple bioaccessibility extraction test (SBET) have been successfully developed and validated to estimate the oral bioaccessibility of elements in soil and dust (Sialelli et al., 2010). SBET is a simplification from PBET and designed to be fast, easy, and reproducible (US EPA, 2008).

Another group of contaminants in street dust are PAHs, which are ubiquitous, semi-volatile, and persistent organic pollutants (POPs) (Jiang et al., 2014; Li et al., 2015; Net et al., 2015). Some are also regarded as priority pollutants (Žibret, 2013). In general, sources of PAHs can be broadly classified into two main groups: pyrogenic and petrogenic, with the pyrogenic group being the dominant sources. The pyrogenic sources include oil derivatives, coal combustion, natural gas, and traffic-related pollution, whereas petrogenic sources consist of direct contamination such as spillage of oil products (Liu et al., 2009). PAHs can accumulate in street dust via atmospheric deposition and may threaten human health if reaching the levels of toxic pollutants (Lorenzi et al., 2011). To reduce the risk associated with PAHs through source control, quantitative understanding of the sources of PAHs is essential (Boonyatumanond et al., 2007).

Human's health risks due to street dust, especially for children are reported frequently (Trujillo-González et al., 2016). Therefore, it is a key scientific issue to study the origin, distribution and level of contaminants in the street dust of urban environments (Zhang et al., 2012). Characterizing the dominant sources of pollutants in road dust is important to aid implementation of suitable management strategies, as well as quantifying the levels of pollution. In addition to the geochemical approaches, multivariate statistical methods, e.g., correlation analysis (CA) and factor analysis (FA) have been widely used in source identification of pollutants in road dust (Yildırım and Tokalıoğlu, 2016).

Mashhad is the second most populous city in Iran (Shaddel and Shokouhian, 2014). During the last few decades, Mashhad metropolitan area has experienced rapid development in urbanization and industrialization, which has in turn exerted a lot of pressure on the urban environment. Several studies of PTEs contamination and source identification of street dusts in some cities of Iran have been carried out (e.g., Saeedi et al., 2012; Soltani et al., 2015; Keshavarzi et al., 2015). However, there is no information available on PTEs and organic contaminants in surface dust of Mashhad city. The objectives of this initial and comprehensive study include 1) assessing the bioaccessibility and levels of selected PTEs: Hg, Mo, Cu, Pb, Zn, Co, Cd, Sb, Mn, Cr, Al and Fe, in dust taken from urban sites having different land uses; 2) investigate the mineralogy and physicochemical characteristics of dust particles; 3) calculate pollution indices to assess the level of pollution as a tool for urban sanitation decision-making; and 4) evaluate the human health risk of selected PTEs and PAHs to both children and adults via inhalation, ingestion as well as dermal contact. The results of this study are valuable for the selection of the urban sweeping vehicles to remove more pollutants in surface dust. In addition, the findings of this research are beneficial for the source control of nonpoint source pollution management and improving environmental quality to promote the health of urbanites in Mashhad Municipality.

2. Materials and methods

2.1. Study area

Mashhad, the capital of Razavi Khorasan Province, with an area of 327 km^2 is located northeast of Iran and close to Turkmenistan and Afghanistan borders. With about 4 million residents and > 20 million tourists and pilgrims, Mashhad is the second largest holy city in the world (Borji et al., 2011). The city is located between 35° 59″ N to 37° 04″ N and 58° 22″ E to 60° 07″ E (Fig. 1), in the valley of the Kashafrud River, between the two mountain ranges of Binalood and Hezar Masjed. Benefiting from proximity to the mountains, Mashhad megacity enjoys cool winters, pleasant springs, mild summers and autumns. Average annual rainfall is 250 mm, some of which occasionally falls as snow. Precipitation generally occurs between December and May (Emamapour et al., 2015).

Geologically, Mashhad plain is a Graben formed between two main tectonic zones of Binaloud in north and Kopeh-Dagh in the south. Mashhad city is built on thick gravel fans and alluvial deposits (Ghazi et al., 2015). However, some ultramafic rocks, loess deposits, calcareous marls, limestone and shale units are also present (Karimi et al., 2017). Mineralogically, the plain is mostly made up of quartz, feldspar, calcite, illite, kaolinite and sericite minerals (Ghazi et al., 2015). Thickness of the alluvial deposits increases towards the east and central parts and exceeds 350 m (Ghazi et al., 2015). The dominant soil types include calcaric cambisols, gypsic regosols, calcaric regosols and calcaric fluvisols covering pediment plains, plateaus and upper terraces and gravelly colluvial fans, respectively (Bagherzadeh and Mansouri-Daneshvar, 2011).

2.2. Sampling, sample preparation and chemical analysis

A total of 22 road dust samples were collected from all over the urban areas of Mashhad with different land uses (commercial, residential, industrial and highway) (Fig. 1). Sampling was carried out in the period July to August 2014. Road characteristics, land use near the sampling sites, and geographic coordinates were recorded. At each site, about 500 g of dust present on impervious surfaces (road, pavement) within an area of 2–10 m^2 were collected using polyethylene brushes. Collected samples were transferred to a sealed polyethylene bag before transport to the laboratory. All the samples were air-dried in the laboratory. Then each sample was sieved through a 2-mm nylon sieve and split into two fractions. The first fraction was used for physico-chemical analysis, whiles the second, was passed through a 63-μm (220 mesh) sieve to obtain the silt and clay fractions for evaluation of total concentration of elements. The mineralogy of dust samples was determined using X-ray diffraction (XRD) at the geological survey of Tabriz, Iran. For this purpose, samples were ground using a Tema Grinder and a Siemens D 500 diffractometer. Total concentrations of 12 PTEs (Hg, Mo, Cu, Pb, Zn, Co, Cd, Sb, Mn, Cr, Al and Fe) were measured following Aqua Regia digestion using inductively coupled plasma mass spectrometry (ICP-MS, PerkinElmer ELAN 9000) at the accredited Acme Analytical laboratory, Canada. For the analysis of PTEs, a wet digestion procedure was adopted (Qi and Gregoire, 2000). Quality control and quality assessment included reagent blanks, analytical duplicates and analysis of the standard reference materials (multi-element soil standard OREAS45EA and OREAS24P). The recovery percentages are Hg (81%), Cr (98.8%), Cu (97.1%), Mn (91.8%), Co (102.3%), Pb (96.6%), Zn (92.5%), Cd (95.6%), Fe (105.7%), Al (101.1%), Mo (95.8%) and Sb (98.3%) indicating a good agreement between the measured and the certified values.

Hydrometric method was used to measure dust particle sizes for sand, silt, and clay according to Gee and Bauder (1986). Dust samples were categorized based on the classification of Shepard (1954) using Rockworks software (version 14). OM content of samples was estimated using the loss on ignition (LOI) method (550 °C for 4 h) (Heiri et al., 2001). Cation exchange capacity (CEC) was determined using sodium acetate and ammonium acetate solution. This method is described by Ryan et al. (2007). Back titration method was implemented to measure the carbonate content. Also, pH_{water} of samples were measured on a 5 g to 25 mL slurry using a pH meter (PHS-3C).

20 street dust samples were also collected and kept in a solvent-cleaned glass jar for 16 quantified PAHs determinations (Fig. 1). The samples were refrigerated (4 °C) during transport to the laboratory of Isfahan University of Technology. In the laboratory, samples were freeze-dried before analysis. An ultrasonic bath (KUDOS, SK3210LHC model) was used during the extraction. Approximately 5 g of each

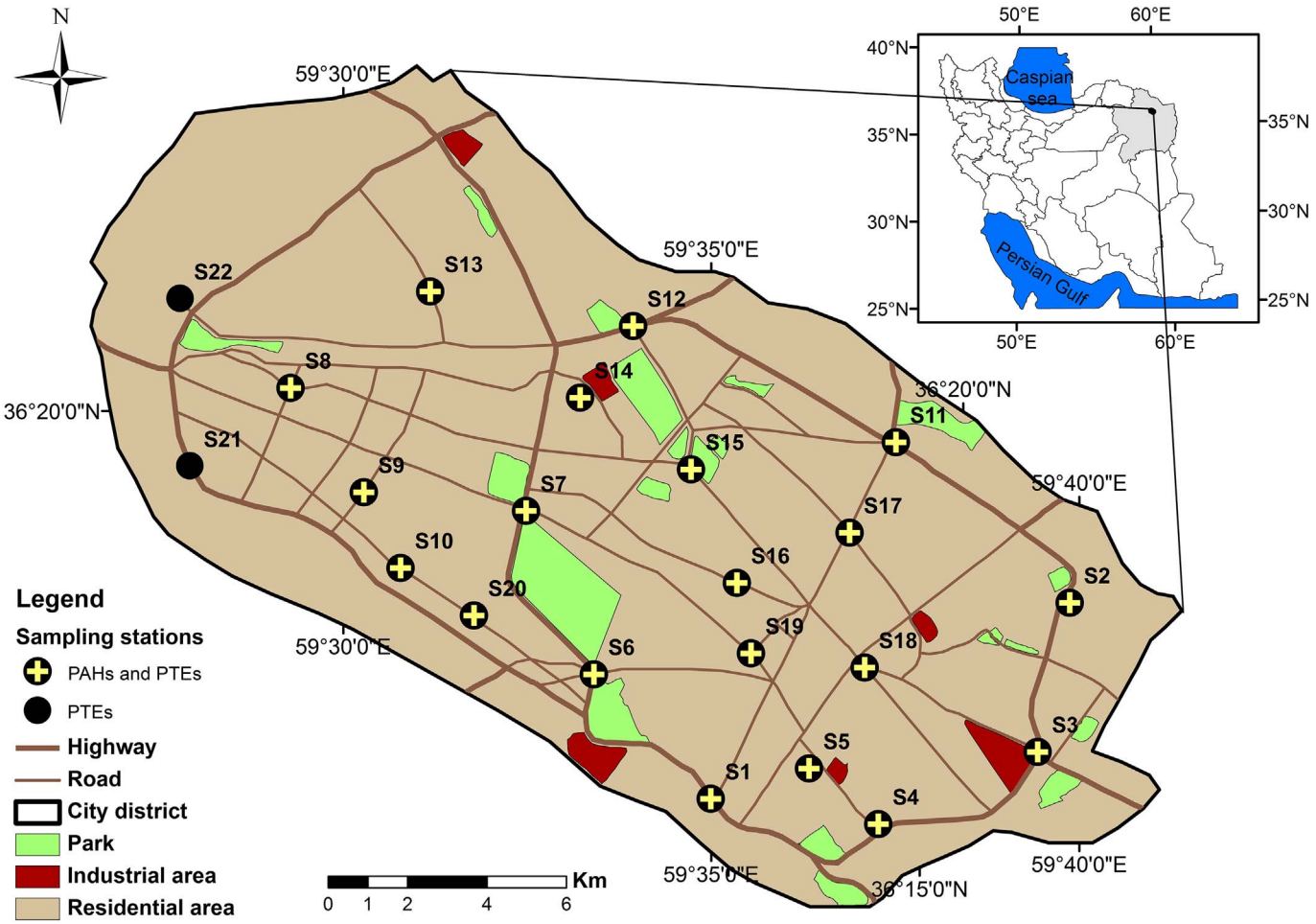

Fig. 1. Study area and sampling sites in Mashhad megacity.

freeze-dried samples was spiked with surrogate standards (Pyrene-D10, lot: 10510 semi-volatile internal standards). The samples were then extracted using a 30-mL mixture of organic solvents (*n*-hexane and dichloromethane [DCM] in a 1:1 v/v) for 30 min at room temperature. The filtered extracts were concentrated to 2 mL by using amorphous sodium sulfate. The last fraction was then analyzed for 16 PAHs (naphthalene (Np), acenaphthene (Ace), fluorene (Fl), phenanthrene (Phe), anthracene (Ant), fluoranthene (Flu), pyrene (Pyr), benzo[*a*] anthracene (BaA), chrysene (Chr), benzo[*b*]fluoranthene (BbF), benzo [*k*]fluoranthene (BkF), benzo[*a*]pyrene (BaP), benzo[*e*]pyrene (BeP), benzo[*ghi*]perylene (BghiP), indeno(1,2,3*cd*)pyrene (IcdP), and dibenz [*a*,*h*]anthracene (DahA)) commonly determined in environmental investigations using gas chromatography/mass spectrometry (Agilent 6890 N GC, 5975C mass selective detector (MSD), USA) equipped with an HP-5MS Capillary column (30 m × 0.32 mm × 0.25 μm, Agilent, USA) in selected-ion monitoring (SIM) mode. The carrier gas was helium at a flow rate of 1.5 mL/min. Oven temperature was initially set at 60 °C (1-min hold) and increased to 295 °C at a rate of 11 °C/min (5-min hold). Mass spectral data, retention times, and peak areas of the calibration standards according to USEPA Methods 8270D and 3550C, 2007, were used for quantification of PAHs.

2.3. Pollution assessment

Geoaccumulation index (I_{geo}) (introduced by Muller, 1981) is a widely used pollution index calculated using the following equation:

$$I_{geo} = \log_2 (C_n / 1.5 B_n) \quad (1)$$

where C_n is the concentration in the road dust samples, and B_n is the background or references concentration. Once the geoaccumulation index is calculated, it can be used to classify the road dust in terms of quality. Muller (1981) proposed seven grades or classes of I_{geo}: class 1 (practically uncontaminated/unpolluted), with I_{geo} values less than zero; class 2 (unpolluted to moderately polluted), with I_{geo} values ranging from 0 to 1; class 3 (moderately polluted), with I_{geo} values from 1 to 2; class 4 (moderately to strongly polluted), with I_{geo} values ranging from 2 to 3; class 5 (strongly polluted), with I_{geo} values from 3 to 4; class 6 (strongly to very strongly polluted), with I_{geo} from 4 to 5; and Class 7 (very strongly polluted), with I_{geo} over 5.

2.4. Simple bioavailability extraction test (SBET)

The detailed standard operating procedure of SBET was described in the report of US EPA (2008), which is used to investigate the relative bioavailability of PTEs. Briefly, bioavailable PTEs measured using SBET was obtained by extracting 0.5 g of samples with glycine (0.4 M; pH = 1.5 readjusted with concentrated HCl) rotated end-over-end for 1 h at 37 °C. The mixture was centrifuged and the supernatant was filtered through Whatman paper number 42. The pH of the filtrate should be within 0.5 pH units of the starting pH, otherwise the procedure has to be redone. The filtrate samples were stored in a refrigerator at 4 °C until analysis. The extractions were conducted in duplicate. Analysis must be performed within one week after in vitro digestion. Concentrations of Pb, Cu, Zn, Mn, Cr, Co, Fe and Al were determined using inductively coupled plasma optical emission spectrometry (ICP-OES, Optima 5300), and the Hg concentration was measured using ICP-MS (Elan 9000) at the Zarazma laboratory, Iran. Cd, Mo and Sb were not detected in any sample of the SBET.

2.5. Risk assessment model

Exposure to street dust PTEs mostly occurs through three main paths: (a) direct ingestion of substrate particles (D_{ing}); (b) inhalation of resuspended particles through mouth and nose (D_{inh}) or through inhalation of vapors (D_{vapour}); and (c) subcutaneous absorption of PTEs in particles adhered to exposed skin (D_{derm}). The dose received through each of the three paths was calculated using Eqs. (2)–(4) (US EPA, 1996). Hg exposure can also occur via inhalation of vapor, which can be expressed by Eq. (5). For carcinogens, the lifetime average daily dose (LADD) for Cd, Cr and Co inhalation exposure route was used in the assessment of cancer risk (US EPA, 1996, 2001).

$$\text{Ding} = C \times \frac{IR_{ing} \times EF \times ED}{BW \times AT} \times 10^{-6} \quad (2)$$

$$\text{Dinh} = C \times \frac{IR_{inh} \times EF \times ED}{PEF \times BW \times AT} \quad (3)$$

$$\text{Dderm} = C \times \frac{SL \times SA \times ABS \times EF \times ED}{BW \times AT} \times 10^{-6} \quad (4)$$

$$\text{Dvapor} = C \times \frac{IR_{inh} \times EF \times ED}{VF \times BW \times AT} \quad (5)$$

$$\text{LADD} = \frac{C \times EF}{AT \times PEF} \times \left(\frac{\text{IRinh}_{child} \times ED_{child}}{BW_{child}} + \frac{\text{IRinh}_{adult} \times ED_{adult}}{BW_{adult}} \right) \quad (6)$$

All parameters are described in Table 1. C (exposure-point concentration, mg/kg) in Eqs. (2)–(6), combined with the values for the exposure factors shown above, is considered to yield an estimate of the "reasonable maximum exposure" (US EPA, 2001), which is the upper limit of the 95% confidence interval for the mean. In this study, the 95% upper confidence limit (UCL) was calculated as shown in Eq. (7) (US EPA, 1996). Calculation of the exposure-point concentration term for log-transformed data:

$$C95\%UCL = \exp.\left\{ X + 0.5 \times s2 + \frac{S \times H}{\sqrt{n-1}} \right\} \quad (7)$$

where X is the arithmetic mean of the log-transformed data, s the standard deviation of the log-transformed data, H the H-statistic and n the number of samples.

In this study, quantified risk or Hazard Indices for both carcinogenic and noncarcinogenic effects was applied to each exposure pathway in the analysis. The doses thus calculated for each element and exposure pathway are subsequently divided by the corresponding reference dose to yield a hazard quotient (HQ), whereas for carcinogens the dose is multiplied by the corresponding slope factor to produce an estimate of cancer risk. Hazard index (HI) is equal to the sum of HQ. The approach assumes that the magnitude of the adverse effect is proportional to the sum of the ratios of the simultaneous sub threshold exposure to acceptable exposure for each chemical (US EPA, 1996). If the value of HI is less than one, it is believed that there is no significant risk of noncarcinogenic effects. If HI exceeds one, then there is a chance that noncarcinogenic effects may occur, with a probability which tends to increase as the value of HI increases (US EPA, 2001).

2.6. PAHs source analysis

PAHs from typical combustion origin are commonly represented by the sum of major combustion specific compounds (ΣComb), which include Flu, Pyr, BaA, Chr, BbF, BkF, BaP, IcdP, and BghiP. The ratio of ΣComb to ΣPAHs (ΣComb/ΣPAHs) is generally used to identify the source of PAHs (Hwang et al., 2003). To avoid a single molecular marker causing susceptible impact of PAHs biodegradation behavior, diagnostic ratios of PAHs were used to distinguish petrogenic and pyrogenic sources of PAHs in street dust of Mashhad. In recent studies on soil and dust PAHs contamination such ratios as BaA/(BaA + Chr), IcdP/(IcdP + BghiP), Flu/(Flu + Pyr), Phe/Ant, Ant/(Ant + Phe) and BaP/BghiP were used to differentiate sources of PAHs (Ray et al., 2008; Wang et al., 2011). In this study ratios of BaA/(BaA + Chr), Flu/(Flu + Pyr) and Ant/(Ant + Phe) were calculated to distinguish PAHs sources.

2.7. Health risk assessment of PAHs

Some PAHs, such as Np, BaA, BbF, BkF, BaP, and DahA, are known to be mutagenic and/or carcinogenic compounds (Lee and Dong, 2010). In this study, the toxicity of each PAH was evaluated separately, based on the set of toxicity equivalency factors (TEFs) proposed by Nisbet and LaGoy (1992) in which BaP is the reference chemical and other PAHs have their own TEF values based on their carcinogenic level relative to that of BaP. The toxic equivalent concentration (TEQ) of each street dust sample was obtained by summing the products of each individual PAH concentration and it's TEF, as follows:

$$TEQ = \Sigma (C_i \times TEF_i) \quad (8)$$

where, TEQ is the toxic equivalent concentration, C_i is the concentration of PAH I, and TEF_i is toxicity equivalency factor of PAH I.

Incremental lifetime cancer risks (ILCRs) associated with exposure to PAHs in Mashhad road dust through the three paths were evaluated as follows (Chen et al., 2013):

$$\text{ILCRsing} = \frac{CS \times \left(CSF_{ing} \times \sqrt[3]{\left(\frac{BW}{70}\right)} \right) \times IR_{ing} \times EF \times ED}{BW \times AT \times 10^{6}} \quad (9)$$

Table 1
Exposure factors for dose models.

Factor	Definition	Unit	Value		Reference
			Children	Adult	
C	Exposure-point concentration	mg/kg	95%UCL		This study
IngR	Ingestion rate	mg/d	200	100	US EPA, 2001
InhR	Inhalation rate	m^3/d	7.6	20	Zheng et al., 2010
PEF	Particle emission factor	m^3/kg	1.36×10^9		US EPA, 2001
SA	Exposed skin area	cm^2	2800	5700	US EPA, 2001
SL	Skin adherence factor	mg cm^{-2} d^{-1}	0.2	0.7	US EPA, 2001
ABS	Dermal absorption factor	Unitless	0.001		Zheng et al., 2010
ED	Exposure duration	year	6	24	US EPA, 2001
EF	Exposure frequency	d/y	180		Zheng et al., 2010
BW	Average body weight	kg	15	70	US EPA, 1996
AT (for non-carcinogenic)	Average exposure time	d	ED × 365		US EPA, 1996
AT (for carcinogenic)			25,550		Zheng et al., 2010
VF	Volatilization factor	m^3/kg	32,675.6		Zheng et al., 2010

$$ILCRsderm = \frac{CS \times \left(CSF_{derm} \times \sqrt[3]{\left(\frac{BW}{70}\right)}\right) \times SA \times EF \times AF \times ABS \times EF \times ED}{BW \times AT \times 10^6} \quad (10)$$

$$ILCRsinh = \frac{CS \times \left(CSF_{inh} \times \sqrt[3]{\left(\frac{BW}{70}\right)}\right) \times IR_{inh} \times EF \times ED}{BW \times AT \times PEF} \quad (11)$$

where CS is the PAHs concentration of dust samples (μg/kg), and CSF is the carcinogenic slope factor (mg/kg day). The determination of carcinogenic slope factor is based on the carcinogenicity of BaP. CSF values for ingestion, dermal and inhalation paths are 7.3, 25 and 3.85 $(mg/kg\ day)^{-1}$, respectively (Chen et al., 2013). Other parameters are presented in Table 1. The risk of cancer for children and adults of different gender was calculated separately. The total risks were calculated as the sum of risks associated with each exposure.

2.8. Data pretreatments

In multivariate statistics and linear geostatistics, a normal distribution for the variables under study is desirable (Webster and Oliver, 2001). Even though normality may not be strictly required, serious violation of normality, such as too high skewness, can impair the reliability of statistical results (Zhang and McGrath, 2004). In this study, the normality of the data was checked using Shapiro–Wilk test ($p > 0.01$). The results show that Pb, Cu, Zn, Cd, Mo, Sb, Hg, Fe and Al concentrations are non-normally distributed in the Mashhad street dust samples (significant level < 0.05). Also, values of standardized skewness and kurtosis indicate significant departures from normality that confirmed these elements are not normally distributed. In numerous data transformation methods, logarithmic transformation is widely applied (Webster and Oliver, 2001). However, it is often found that environmental variables do not always follow the lognormal distribution (Zhang and McGrath, 2004). In our study, the Box-Cox transformation was used to make the data more normal and less skewed using SPSS 21 software package.

2.9. Statistical analysis

To identify the relationship among PTEs and PAHs in road dust and their possible sources, Pearson's correlation coefficients and factor analysis (FA) were performed using the commercial statistics software package SPSS version 21 for Windows. The correlation coefficient measures the strength of inter-relationship between two PTEs or PAHs. In environmental science, FA is a useful statistical tool that can extract latent information from multidimensional data and group it into fewer ones (Keshavarzi et al., 2017). Kaiser-Meyer-Olkin (KMO) and Bartlett's tests were used for checking the interest of the implementation of the FA on dataset. The KMO measure of sampling adequacy indicates whether the partial correlations among items are small. Bartlett's test of sphericity indicates whether the correlation matrix is an identity matrix, which in turn reveals that the factor model is inappropriate. In this study, the values for KMO and Bartlett's tests were 0.72 (> 0.6) and 0.00 (< 0.05) respectively, indicating good conditions for using FA.

3. Results and discussion

3.1. General dust properties

The physicochemical characteristics of street dust samples are outlined in Table 2. Values of pH ranging in a narrow interval (7.3–9.8), which suggests subalkaline conditions for all samples because of the high calcium carbonate contents of the analyzed dusts from 7.6 to 21%, with an average value of 11.8%. The excessive inputs of sub-alkaline building materials (e.g., cement and calcareous) into the urban topsoil and street dust may have resulted in dust alkalization especially in residential areas (Al-Khashman and Shawabkeh, 2006). Based on the Shepard textural classification, Mashhad dusts texture could be classified as sandy clay loam and clay loam which shows the dominance of sand and clay particles. Sand particles were found to be dominant in all samples (30.6–70.6%) followed by clay (20.2–34.5%) and silt (5.6–38.3%). The dust organic matter level ranged from 1.23 to 11%. Fergusson and Ryan (1984) estimated the organic matter content of street dust from different city types, ranging from 3.5 to 18.3%, by ignition at 500 °C for 16 h. Al-Chalabi and Hawker (1996) reported a mean organic matter content of 4.1% in their samples (ignition at 500 °C for 12 h). In general, the results of this study fall within the ranges of previous studies. The dust samples in S5, S7, S12, S15, S16 and S18 stations display the highest OM content (Table 2). Also, Table 2 shows that the highest CEC values occur in S3, S8, S9, S12, S15, S16, S18, S20 and S21 stations. Therefore, both clay size particles and OM content play a significant role in dust's CEC. In the study area, CEC varies between 12.4 and 55 meq/100 g. Following the Metson (1961) classification, the samples of the study area can be categorized as dust with very high CEC values. Given the high CEC value and carbonate content, the dust samples have a high capacity to retain PTEs through adsorption mechanisms.

3.2. Dust mineralogy

The results of X-ray diffractometry indicated that Calcite (also Mg-Calcite), Dolomite, and Quartz (also α-quartz) are dominant minerals in all sampling sites. Lower abundances of Rutile (TiO_2), Anatase (TiO_2) (one of the three rarer polymorphs of TiO_2) and Montmorillonite occur in some samples. According to Salmanzadeh et al. (2015), the similarity of mineralogical composition particularly major phases in dust samples indicate that they should have majorly originated from similar sources. The abundance of quartz is due to resistance to chemical and physical weathering, which allows it to persist over long periods of erosion and transport. The abundance of calcite reflects local geology of the study area (Amrhein and Suarez, 1987). In general, the mineralogy of surface dust is controlled by regional geology and wind direction. Comparison of the mineralogy of dust samples with the geology of study area suggests that geological formations and composition of the soils of surrounding Mashhad metropolitan city should have a direct impact on the mineralogical composition and chemistry of the dust samples.

3.3. PTEs concentrations in dust samples

Descriptive statistics of PTEs concentrations in the street dust of Mashhad as well as background values of upper continental crust (Rudnick and Gao, 2003) are presented in Table 3. For major elements (e.g. Fe, Al and Mn), conversion factors were used to convert oxides to elements (1.286 for Fe, 1.291 for Mn and 1.889 for Al) (SGS, 2014). Table 3 reveals that average concentration of Cu (112.8 ± 67.7 mg/kg), Pb (100.5 ± 58 mg/kg), Zn (325.8 ± 125.4 mg/kg), Cd (0.3 ± 0.09 mg/kg), Mo (2.8 ± 1.6 mg/kg), Sb (3.1 ± 1.8 mg/kg), and Hg (430 ± 630 μg/kg) in Mashhad road dust samples is higher than corresponding concentrations in the upper continental crust. The results show significant heterogeneity in their chemistry reflected by high standard deviation and coefficients of variation (CV = standard deviation/mean) (Table 3). From a statistical stand point, the property is considered highly variable and dispersed when the CV exceeds 0.3 (Mashal et al., 2015). Thus, the dust samples exhibited great variations in the concentrations of Cu, Pb, Zn, Cd, Hg, Mo and Sb (Table 3). Except for Co and Mn, skewness for all PTEs is positive showing that mean concentrations are higher than their median concentration. Skewness and kurtosis values for Cu, Mo and Hg were higher than other elements, which indicate the existence of highly contaminated spots. The

Table 2
Selected physicochemical properties of Mashhad street dust samples.

Station	pH	CEC (meq/100 g)	OM (%)	Ca. carbonate (%)	Sand (%)	Silt (%)	Clay (%)	Texture
S1	7.27	16.48	6.18	20.97	70.56	5.64	23.8	Sandy clay loam
S2	9.32	13.96	4.60	13.29	58.84	19.28	21.88	Sandy clay loam
S3	9.70	33.75	7.35	7.61	62.56	12.28	25.16	Sandy clay loam
S4	8.83	14.85	3.01	16.66	50.2	22.64	27.16	Sandy clay loam
S5	8.21	15.60	9.20	8.21	60.56	19.28	20.16	Sandy clay loam
S6	8.94	13.10	6.33	9.08	57.84	15.36	26.8	Sandy clay loam
S7	9.04	15.64	8.16	11.87	62.12	13.36	24.52	Sandy clay loam
S8	8.70	44.52	4.86	11.16	54.2	16.64	29.16	Sandy clay loam
S9	9.31	20.45	5.30	10.44	60.56	15.28	24.16	Sandy clay loam
S10	8.46	14.20	7.94	12.62	48.56	25.28	26.16	Sandy clay loam
S11	9.32	17.06	6.21	13.61	56.56	18.56	24.88	Sandy clay loam
S12	8.81	23.80	9.57	9.23	44.84	20.64	34.52	Clay loam
S13	9.29	13.16	5.37	15.22	48.84	16.92	34.24	Sandy clay loam
S14	9.78	13.60	3.54	12.25	56.56	22.92	20.52	Sandy clay loam
S15	8.90	22.19	9.44	12.57	57.56	19.92	22.52	Sandy clay loam
S16	8.41	54.90	8.37	11.88	43.12	26.36	30.52	Clay loam
S17	9.51	15.79	7.57	11.42	58.2	15.64	26.16	Sandy clay loam
S18	9.48	41.71	10.97	9.79	30.56	38.28	31.16	Clay loam
S19	9.31	12.39	5.43	13.49	62.56	10.28	27.16	Sandy clay loam
S20	8.89	29.04	7.26	9.76	50.56	22.92	26.52	Sandy clay loam
S21	9.41	30.23	2.92	9.66	45.12	26	28.88	Sandy clay loam
S22	8.61	13.24	1.23	8.32	66.84	6.92	26.24	Sandy clay loam
Min	7.27	12.39	1.23	7.61	30.56	5.64	20.16	–
Max	9.78	54.90	10.97	20.97	70.56	38.28	34.52	–
Mean	8.98	22.26	6.40	11.78	54.88	18.64	26.47	–
Median	8.99	16.13	6.27	11.64	57.06	18.92	26.2	–

maximum contents of Sb, Pb, Zn, Cu and Hg were detected in samples taken from the most heavily traffic-loaded areas (e.g. Abbaspour square, Kushesh street, Azadi square, Abutaleb street and Underpass of the holy shrine).

Direct comparison of PTE concentrations in the urban street dust among different cities is approximate due to different sampling methods, differences in sample digestion and used analytical methods (Lu et al., 2016). However, some general conclusions regarding dust contamination of cities with PTEs can be drawn from such a comparison. Therefore, in this study, minimum, maximum and mean concentrations of PTEs in Mashhad road dust are compared with data reported for other cities around the world (Table 4). In order to reveal the similarities and differences, the granulometric fraction and the used chemical method for analysis of PTEs are also presented. It is already known that the concentration of PTEs in urban street dust particles vary considerably among cities depending on the population density, traffic load, traffic congestion, industrial activities, technologies employed, geological setting, as well as local weather conditions and wind patterns (Soltani et al., 2015). In general, dust elemental concentrations were of relatively moderate pollution degree compared with the concentrations reported for other cities. Hg in road dust from Mashhad was higher than in other cities except for Shiraz (Iran) and Baoji (China), probably due to more industrial activities in Mashhad. The mean concentration of Mo in Mashhad road dust was low compared to several cities around the world except for Luanda (Angola) and Nanjing (China). Cd concentrations in Mashhad street dust were almost similar with those in Shiraz and Thessaloniki (Greece); lower than Monterrey (Mexico), Luanda, Tehran and Isfahan (Iran); and higher than Toronto (Canada), reflecting the presence of strong point sources. The mean concentration of Sb in this study is lower than all other compared cities in the world. The Co Concentration in the present study is much higher than for all other presented cities, except for Isfahan and Baoji. Also, Zn had lower concentrations in Mashhad compared with the other cities except for Toronto and Luanda. Compared with PTEs contents in other cities, the mean concentration of Pb in the present study is lower than all other cities, except for Isfahan. This could be attributed to heavier traffic in these cities. Mean concentration of Cu in Mashhad street dust was only higher than Luanda. Detailed comparisons are clearly presented in Table 4.

I_{geo} is used to assess the degree of dust contamination by PTEs. In this study, I_{geo} was calculated using upper continental concentrations (Rudnick and Gao, 2003). The I_{geo} for Hg, Cu, Mo, Co, Al, Cd, Pb, Sb,

Table 3
Descriptive statistics of PTEs concentration in dust samples together with recommended composition of the upper continental crust.

Element	Minimum	Maximum	Mean (SD)[a]	Median	CV	Skewness	Kurtosis	Upper continental crust[b]
Pb (mg/kg)	26.09	263.39	100.48 (57.98)	76.96	0.58	1.51	1.82	17.00
Cu (mg/kg)	33.71	368.91	112.79 (67.70)	95.64	0.60	2.78	9.85	28.00
Zn (mg/kg)	107.40	698.70	325.79 (125.36)	309.45	0.38	1.21	2.73	67.00
Co (mg/kg)	8.30	12.80	10.56 (1.05)	10.65	0.10	−0.21	0.47	17.30
Cd (mg/kg)	0.18	0.56	0.30 (0.09)	0.29	0.30	1.19	1.78	0.09
Mo (mg/kg)	0.90	7.93	2.87 (1.53)	2.55	0.54	2.12	5.34	1.10
Sb (mg/kg)	1.19	8.06	3.24 (1.79)	2.99	0.55	1.21	1.32	0.40
Mn (mg/kg)	372.00	588.00	480.23 (44.46)	481.00	0.09	−0.10	1.59	1000.00
Cr (mg/kg)	55.10	133.80	85.63 (19.19)	80.90	0.22	1.01	1.08	92.00
Hg (μg/kg)	14.00	2403.00	431.95 (629.34)	127.00	1.46	1.99	3.83	50.00
Fe (mg/kg)	19,200.00	35,700.00	25,109.09 (3843.97)	24,500.00	0.15	1.16	1.56	35,000.00
Al (mg/kg)	7900.00	16,000.00	11,081.82 (1439.46)	10,950.00	0.13	1.51	6.81	84,700.00

[a] Arithmetic mean and standard deviation in parenthesis.
[b] Rudnick and Gao (2003).

Table 4
A comparison of PTEs contents (minimum-maximum (mean)) in street dust of different cities (mg kg^{-1} except for Hg in μg kg^{-1}).

City	Fraction	Chemical method	Mo	Hg	Cd	Cr	Cu	Fe	Mn	Co	Pb	Sb	Zn
Mashhad (This study)	< 63 μm	ICP-MS	0.9–7.9 (2.9)	14–2403 (432)	0.2–0.6 (0.3)	55–134 (86)	34–369 (113)	19,200–35,700 (29109)	372–588 (480)	8.3–12.8 (10.6)	26–263 (100.5)	1.2–8.1 (3.2)	107.4–699 (326)
Shiraz (Iran)[a]	< 63 μm	ICP-MS	1.9–6.4 (4.1)	4–4504 (1050)	0.3–0.9 (0.5)	31.6–106 (67.2)	49.8–232.5 (136.3)	16,300–24,900 (20,254.6)	245–652 (438.5)	6.1–13.4 (8.7)	36.8–234.3 (115.7)	0.8–9.5 (4.8)	161–778 (403.5)
Tehran (Iran)[b]	< 63 μm	ICP-MS	–	–	9.9–11.1 (10.7)	15.2–58 (33.5)	68.3–778.3 (225.3)	26,602.5–96,427.3 (47,935.7)	721.6–2231.6 (1214.5)	–	64.7–764.9 (257.4)	–	544.3–1935.2 (873.2)
Isfahan (Iran)[c]	< 63 μm	ICP-MS	–	–	0.5–7.9 (2.1)	59–104 (82.13)	55.4–955.5 (182.3)	25,500–118,500 (39800)	577–2455 (876.4)	10.6–19.1 (13.9)	12.2–61.2 (46.8)	1.85–24.2 (6.9)	212.4–2319 (707.2)
Nanjing (China)[d]	< 63 μm	ICP-OES	–	50–340 (120)	0.4–2.2 (1.1)	60.6–250 (126)	28.7–272 (123)	17,900–66,000 (34200)	382–1294 (646)	6.7–20.7 (10.7)	37.3–204 (103)	–	140–798 (394)
Baoji (China)[e]	< 75 μm	XRF, AFS	–	500–2300 (1100)	–	98.9–214.5 (126.7)	77.9–259.9 (123.2)	–	544.5–2335.8 (804.2)	12.6–22.9 (15.9)	151.9–1969.8 (433.2)	–	384.9–1778.3 (715.3)
Toronto (Canada)[f]	< 2 μm	AAS	–	–	0.1–0.5 (0.2)	57.3–558 (197.9)	53.9–392.1 (162.2)	1474–70,050 (48,234.5)	100–3125 (1407.2)	–	32.5–378.7 (182.8)		39.3–1367.8 (232.8)
Thessaloniki (Greece)[g]	< 250 μm	ICP-MS	2.6–13.8 (6.1)	–	0.2–1 (0.6)	43–307 (187.3)	125.5–1667 (526.2)	6100–39,100 (25100)	372–781 (529.1)	5.2–14.5 (9.6)	56–492.3 (191)	5.5–24.7 (12.6)	154–2153 (671)
Witbank (South Africa)[h]	< 125 mm	ICP-MS	1.0–12.5 (2.8)	5–1710 (92)	0.1–0.9 (0.2)	299–43,000 (5250)	13.8–300.3 (73.2)	20,000–173,700 (62900)	610–20,000 (2264)	7.1–63.9 (24.2)	10.8–835 (89.3)	0.3–7.2 (1.9)	32–1330 (222)
Celje (Slovenia)[i]	< 125 mm	ICP-MS	1.2–43.3	–	0.4–7.2	15–740	29–295	79,000–127,000	197–2970	3–15.3	15–352	1.2–7.3	88–2220
Monterrey (Mexico)[j]	< 63 μm	AAS	–	–	1.1–13.1 (7.5)	4–335 (78)	–	–	–	–	151–612 (300)	–	32–1024 (475)
Luanda (Angola)[k]	< 100 μm	ICP-MS	1.2–6.3 (2)	30–570 (130)	0.7–4 (1.1)	17–37 (26)	18–118 (42)	8000–20,100 (11572)	157–728 (258)	1.9–7 (2.9)	74–1856 (351)	1.1–37 (3.4)	142–1412 (317)
Amman (Jordan)[l]	< 63 μm	ICP-MS	–	–	2.5–3.4	3.7–19 (11.9)	175–325 (241.7)	4275–9125 (6233)	137.5–167.5 (147.5)	–	219–373	–	250–525 (408.3)

[a] Keshavarzi et al. (2015).
[b] Saeedi et al. (2012).
[c] Soltani et al. (2015).
[d] Hu et al. (2011).
[e] Lu et al. (2010).
[f] Nazzal et al. (2014).
[g] Bourliva et al. (2016).
[h] Žibret et al. (2013).
[i] Žibret (2012).
[j] Valdez Cerda et al. (2011).
[k] Ferreira-Baptista and De Miguel (2005).
[l] Jiries et al. (2001).

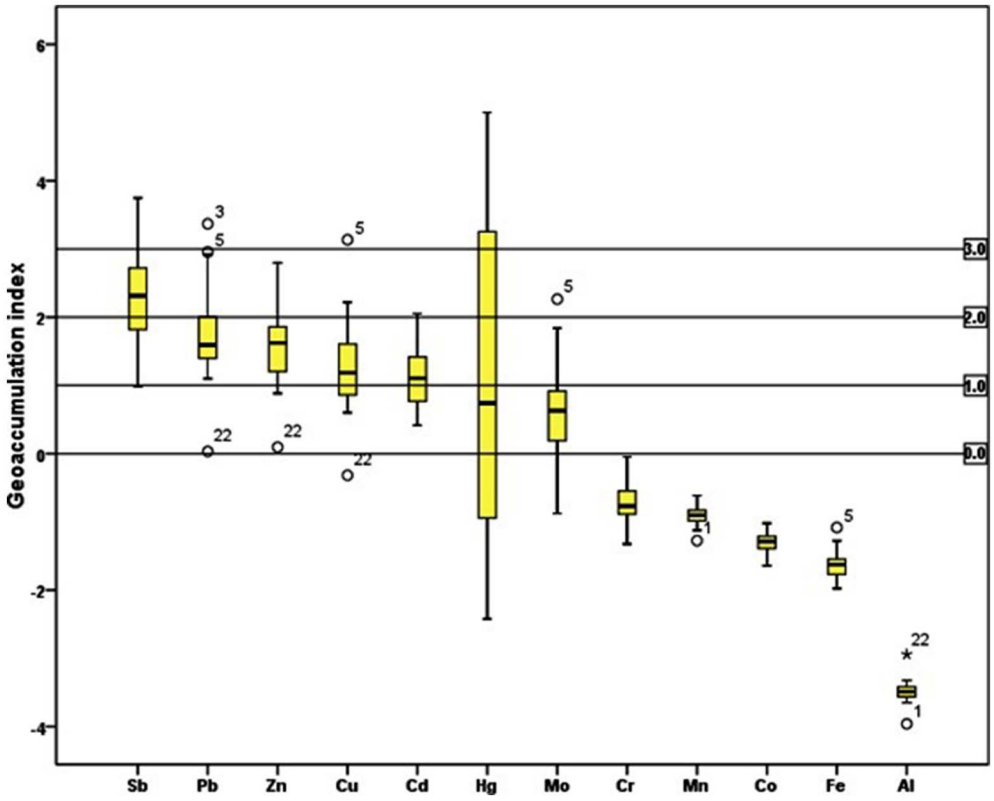

Fig. 2. Box-plot of index of geoaccumulation (I_{geo}) for dust samples.

Mn, Fe, Cr and Zn are indicated in Fig. 2. According to I_{geo}, the degree of contamination displays the following decreasing trend: Sb > Pb > Zn > Cu > Cd > Hg > Mo > Cr ≈ Mn ≈ Co ≈ Fe > Al. The results indicate that some dust samples are very highly to moderately polluted by Pb, Sb, Hg, Cu, Mo, Zn and Cd. Also, according to calculated I_{geo}, the lowest contamination degree belongs to Al, Co, Mn, Cr, and Fe. It is obvious that I_{geo} variations are greater in the first seven elements, especially for Hg (Fig. 2). Hg in 23.3% of the stations is placed in "strongly polluted" category ($I_{geo} \geq 3$). Samples at station 5, a high traffic area with many industrial workshops, are moderately to strongly polluted with Sb, Pb, Zn, Cu, Mo and Hg displaying an I_{geo} value > 2. Instead, the I_{geo} values for Hg, Mo, Zn, Cu, Pb and Sb in station 22 with light traffic and no industrial plants, fall within the range of unpolluted to moderately polluted. These findings indicate that traffic load and industrial activities have a considerable effect on pollution degree of road dust.

To investigate the interrelationships between variables in road dust samples, the Pearson's correlation matrix was calculated and the result is presented in Table 5. Generally speaking, the correlation between contaminated elements is evident. Pb significantly correlates with Cu (r = 0.82), Zn (r = 0.61), Mo (r = 0.74), Cr (r = 0.68), and Sb (r = 0.54) at 0.01significance level. In general, Correlation analysis shows a strong positive correlation between Zn, Sb, Cu, Mo, and Pb. Similarly, Co, Fe, Al, and Mn in road dust samples are markedly positively correlated. Tumuklu et al. (2007) suggested that PTEs with high and medium positive correlation probably come from the same source. The observed correlations suggest a close link with PTEs origin and common geochemical characteristics. On the contrary, Hg and Cd show no significant positive correlation with any other elements, suggesting a different local source (Table 5).

Source identification of PTEs is critical for pollution prevention and human health protection. FA was applied to identify sources of PTEs in the street dust by applying varimax rotation with Kaiser Normalization. The number of significant factors and the percent of variance were

Table 5
Pearson's correlation coefficients for PTEs in road dust samples of Mashhad (significant correlation values are shown in bold).

Elements	Pb	Cu	Zn	Co	Cd	Mo	Sb	Mn	Cr	Hg	Fe	Al
Pb	1.000											
Cu	**0.816****	1.000										
Zn	**0.612****	**0.680****	1.000									
Co	0.285	0.129	0.232	1.000								
Cd	0.388	0.395	0.265	0.002	1.000							
Mo	**0.744****	**0.856****	**0.809****	0.225	0.323	1.000						
Sb	**0.536****	**0.673****	**0.809****	0.008	0.053	0.809**	1.000					
Mn	0.188	0.255	0.098	**0.646****	−0.123	0.185	0.033	1.000				
Cr	**0.685****	**0.631****	0.497*	0.452*	0.267	**0.615****	0.435*	0.211	1.000			
Hg	0.471*	0.454**	0.354	0.035	**0.566**	0.451*	0.359	−0.042	0.430*	1.000		
Fe	0.492**	0.368**	0.360	**0.626****	0.004	0.478*	0.261	**0.819****	0.473*	0.153	1.000	
Al	−0.010	0.066	0.059	0.491*	−0.345	−0.024	0.015	**0.637****	0.003	0.135	**0.576**	1.000

** Correlation is significant at the 0.01 level (2-tailed).
* Correlation is significant at the 0.05 level (2-tailed).

Table 6
Rotated component matrix for data of Mashhad street dust (principal factors ≥0.6 are bold in each column).

Elements	Factors			Communalities
	1	2	3	
Pb	**0.631**	0.137	0.538	0.58
Cu	**0.781**	0.142	0.522	0.77
Zn	**0.801**	−0.149	0.277	0.89
Co	0.143	**0.874**	0.142	0.68
Cd	0.117	−0.042	**0.843**	0.72
Mo	**0.843**	0.072	0.453	0.56
Sb	**0.864**	−0.086	0.022	0.87
Mn	−0.066	**0.972**	−0.041	0.88
Cr	**0.702**	0.214	0.371	0.83
Hg	0.168	0.082	**0.660**	0.42
Fe	0.334	**0.749**	0.448	0.83
Al	−0.187	**0.819**	−0.454	0.63
Total Eigenvalues	5.4	3.0	1.1	
% of variance	35.4	25.5	17.3	
Cumulative %	35.4	60.9	78.2	

calculated by extracting the eigenvalues and eigenvectors from the correlation matrix. Table 6 shows the results of the factor loadings with a varimax rotation, as well as the eigenvalues and communalities. The results indicate that there were three eigenvalues higher than one and that these three factors explain 78.2% of the total variance. Pb, Cu, Zn, Mo, Cr and Sb exhibited high values in F1, explaining 35.4% of the total variance. As already mentioned, dust samples are moderate to very strongly polluted with Pb, Cu, Zn, Sb and Mo. Also, the dust samples exhibited great variations in the concentrations of these elements (Table 3). These PTEs concentrations in urban areas are reported to be significantly higher than in the suburbs (Tang et al., 2013). The results indicate that Factor 1 can be considered an anthropogenic component. The analyzed PTEs appeared to be multi-source related and their accumulation is thought to be anthropogenic and from traffic-related materials, such as brake dust, tire tread, and street paint. Major fossil fuels combusted in Mashhad are petrol, burned by vehicles. The maximum concentrations of Pb, Zn, Sb, Mo and Cu were found in dust samples collected from high traffic density sites. For instance, Cu, Zn, Mo and Sb can originate from corrosion of alloys used in vehicle components, vehicle covers or other metallic surfaces and materials (Wei et al., 2010). Previous studies (Sezgin et al., 2004; De Miguel et al., 1997) have suggested that the main sources of Pb in street dust are fuel additives and combustion.

Factor 2, mainly included Co, Mn, Al and Fe and accounted for 25.5% of the total variance. The concentrations of these elements in dust samples are close to the corresponding background values and suggested that they mainly come from weathered soil rather than human activity. The I_{geo} values for these elements are low (Fig. 2). Also, standard deviation and coefficients of variation for these elements are minimum among all elements, probably reflecting natural sources such as re-suspension of soil-derived particles.

The third factor was loaded primarily by Cd and Hg, accounting for 17.3% of the total variance. The concentration of these elements was higher than reference values (Table 3). Also, large standard deviations were found in Hg and Cd levels. A significant positive correlation was found between Hg and Cd ($r = 0.566$, $p < 0.01$) (Table 5). Hg and Cd concentrations in excess of the mean were found in dust samples from the industrial area. Thus the third factor may have originated mainly from industrial activities. Many industries including cement manufacturing plants, electric and electronics, food and textile plants are built in suburbia of Mashhad city. Previous studies (Zheng et al., 2010; Saeedi et al., 2012) have revealed that industrial activities, paints, and electrical workshops are the main sources of Cd and Hg in the dust samples.

SBET results can indicate the amount of contaminants which can be absorbed via the ingestion of soils and other similar media (Wang et al., 2007). Bioaccessibility was expressed as the percentage of the element content extracted by SBET with respect to its total content in street dust (Table 7). Among the measured elements, Zn, Pb, Hg, Cu and Mn showed higher bioaccessibility, and Zn demonstrated the highest value (68.5%) in dust samples. The SBET results reveal the following order based on mean values: Zn > Pb > Hg > Cu ≈ Mn > Cr > Co > Fe > Al, suggesting that there were great differences of element bioaccessibility among these studied elements. Table 7 indicates that the highest SBET values for Zn, Hg, Cu, Cr and Pb were found in the industrial areas. The one sample *t*-test was used to compare mean values of SBET in the high traffic, residential and industrial areas. The results show that significant differences exist on the bioaccessibility for Pb, Zn, Hg, Cu, Cr and Co among different land use districts ($p < 0.05$) (Table 7).

Exposure doses of PTEs in the street dust of Mashhad for both children and adults were calculated and the results of the hazard quotient (HQ) values of different exposure pathways and hazard index (HI) of the elements are presented in Table 8. The results indicate that the non-carcinogenic effects for children are higher than for adults. More specifically, the HQs for children through ingestion were averaged 2–6 times higher than those for adults. Also, ingestion appears to be the major route of exposure to street dust for both adults and children, followed by dermal contact except for Fe and Mn. Therefore, the potential health risk through inhalation is almost negligible compared with other exposure routes. This result is also consistent with earlier investigations (Ferreira-Baptista and De Miguel, 2005; Zheng et al., 2010). For non-cancer effect, inhalation of mercury vapor is the main route of exposure in all of the exposure pathways, which was consistent with the study of Fang et al. (2011) and Meza-Figueroa et al. (2007). This is due to the significant vapor pressure of Hg at ambient temperature (Sun et al., 2013). Considering non-carcinogenic effects for children i.e., HI values for the studied PTEs decrease in the order of Hg > Pb > Cr > Cu > Zn > Mn > Co > Fe > Sb > Cd (Table 8). For both adults and children, Hg and Pb had the highest risk values (0.166 for Hg and 0.111 for Pb) whereas Cd has the lowest value (0.000205). However, HI values for all studied elements were lower

Table 7
Bioaccessibility of PTEs (as a percentage of SBET-extractable content to total content) in the studied street dust samples.

Station		Pb	Cu	Zn	Mn	Cr	Hg	Fe	Co	Al
High traffic	Mean	50.2	45.5	60.9	33.4	17.8	43	5.5	10.6	6.4
	SD	8.3	9.2	4.2	10.1	7.3	9.4	3.5	4.1	2.5
Residential	Mean	39.4	27.3	46.2	37.6	15.1	28.8	5.4	6.5	4.2
	SD	3.4	6.5	7.8	8.2	5.7	5.7	2.2	6.2	1.8
Industrial	Mean	48.6	39.8	54.6	40.8	16.9	54.2	7.1	8.4	3.7
	SD	5.9	7.4	6.1	5.5	8.8	8.1	4.8	3.7	0.8
All dust samples	Mean	46.1	37.5	53.9	37.3	16.6	42	6	8.5	4.8
	SD	7.52	8.3	6.87	6.62	5.1	10.7	2.5	3.27	1.18
	Minimum	32.9	18.5	39.2	31.6	12.7	9.9	3.7	5.7	2.8
	Maximum	57.6	52.9	68.5	53.1	27.3	62.6	10.1	12.2	8

Table 8
Hazard quotient and risk for each element and exposure pathway.

Toxic elements	Hg	Pb	Cd noncanc.	Cd canc.	Zn	Cu	Co	Co canc.	Cr noncanc.	Cr canc.	Fe	Sb	Mn
C (95% UCL)	0.493	161.71	0.42	0.42	382.85	133.43	16.89	16.89	96.37	96.37	31,352.3	5.82	601.33
RfDing	3.00×10^{-4}	3.50×10^{-3}	1.00×10^{-3}		3.00×10^{-1}	4.00×10^{-2}	2.00×10^{-2}		3.00×10^{-3}		8.40	5.60×10^{-1}	1.40×10^{-1}
RfDderm	2.10×10^{-5}	5.25×10^{-4}	1.00×10^{-5}		6.00×10^{-2}	1.20×10^{-2}	1.60×10^{-2}		6.00×10^{-5}		7.00×10^{-2}	1.10×10^{-1}	3.50×10^{-3}
RfDinh	8.75×10^{-5}	3.50×10^{-3}	5.00×10^{-5}		3.00×10^{-1}	4.02×10^{-2}	5.71×10^{-6}		2.86×10^{-5}		2.20×10^{-4}		2.60×10^{-2}
Inhal. SF				6.3				9.8		42			
Children													
HQing	2.75×10^{-2}	1.06×10^{-1}	2.01×10^{-3}		8.68×10^{-3}	4.18×10^{-2}	4.47×10^{-3}		4.21×10^{-2}		2.88×10^{-3}	3.08×10^{-3}	7.10×10^{-3}
HQderm	6.58×10^{-6}	4.72×10^{-3}	1.48×10^{-4}		9.23×10^{-5}	5.40×10^{-4}	2.32×10^{-4}		3.14×10^{-3}		1.09×10^{-4}	8.41×10^{-8}	8.90×10^{-9}
HQinh	1.18×10^{-3}	4.47×10^{-5}	1.83×10^{-7}		3.50×10^{-6}	6.52×10^{-7}	1.84×10^{-7}		1.84×10^{-4}		1.65×10^{-3}	2.53×10^{-5}	6.40×10^{-5}
HQvapor	1.37×10^{-1}												
HI = ΣHQi	1.66×10^{-1}	1.11×10^{-1}	2.16×10^{-3}		8.78×10^{-3}	4.23×10^{-2}	4.70×10^{-3}		4.54×10^{-2}		4.64×10^{-3}	3.11×10^{-3}	7.16×10^{-3}
Carcinogenic risk				2.68×10^{-10}				4.13×10^{-8}		4.48×10^{-6}			
Adults													
HQing	1.38×10^{-2}	2.88×10^{-2}	1.59×10^{-4}		4.16×10^{-4}	3.18×10^{-2}	6.23×10^{-4}		5.34×10^{-3}		3.14×10^{-4}	9.50×10^{-4}	5.70×10^{-4}
HQderm	3.09×10^{-6}	2.15×10^{-3}	4.60×10^{-5}		6.25×10^{-6}	4.40×10^{-4}	5.07×10^{-5}		8.06×10^{-4}		6.26×10^{-5}	7.70×10^{-8}	6.41×10^{-10}
HQinh	6.84×10^{-4}	2.77×10^{-6}	1.07×10^{-7}		9.40×10^{-7}	6.52×10^{-7}	8.94×10^{-8}		5.37×10^{-5}		1.18×10^{-5}	6.44×10^{-6}	8.60×10^{-6}
HQvapor	1.04×10^{-1}												
HI = ΣHQi	1.18×10^{-1}	3.10×10^{-2}	2.05×10^{-4}		4.23×10^{-4}	3.22×10^{-2}	6.74×10^{-4}		6.20×10^{-3}		3.88×10^{-4}	9.57×10^{-4}	5.79×10^{-4}
Carcinogenic risk				2.68×10^{-10}				4.13×10^{-8}		7.03×10^{-7}			

than the safe level of 1. However, it should not be overlooked in Mashhad urban street dust due to cumulative manner of some PTEs (for example Hg and Pb) and exposure frequency to the PTEs.

Carcinogenic risk due to urban street dust exposure to Cd, Co and Cr were assessed through the ingestion exposure modes. The carcinogenic risk level for these three PTEs were all low to 10^{-6} magnitude with higher values for Cr (7.03×10^{-7}) followed by Co (4.13×10^{-8}) and Cd (2.68×10^{-10}). Thus, the carcinogenic risk for these elements were all lower than the internationally accepted precautionary criterion (10^{-6}) (Granero and Domingo, 2002), which indicates that the carcinogenic risk of Cd, Co and Cr due to urban street dust exposure is acceptable in Mashhad.

The results showed that exposure to PTEs in street dust would not cause serious health impacts in the study area. However, there is a high degree of uncertainty about the calculated health risk due to exposure to PTEs from street dust. First, the assumptions applied in the models seem too ideal. Second, there were uncertainties regarding the exposure parameters and the elemental toxicity data. Finally, other elements and potential exposure routs (i.e., contaminated soil or indoor dust, etc.) were not considered in this study. It should be noted that this assessment only considered one urban medium (dust). In fact, PTEs pollutants can enter human body via various routs such as food, water, and atmosphere. Therefore, the exact HIs for the inhabitants should be higher. Therefore, the ecological and health effects of the enriched Hg in Mashhad metropolitan city need further detailed investigations. However, though there are some uncertainties, this model has proved to be a useful tool to assess human health risk due to exposure to pollutants in urban environments and could help to supply referenced information for the public or government about the potential risks associated with exposure to PTEs.

3.4. PAHs concentration and distribution in dust samples

In this study, 16 USEPA priority PAHs were detected in all dust samples. The measured data is statistically analyzed and presented in Table 9. The highest average concentration for PAH species in Mashhad street dust belongs to Pyr with 598 μg kg^{-1} followed by Phe, Flu, Chr, and BaA with average levels of 418, 370.9, 199.3 and 150 μg kg^{-1}, respectively. Therefore, Pyr, Phe, Flu, Chr and BaA are the major components of Mashhad dust. These PAHs species are indicative of combustion (Hwang et al., 2003). Meanwhile, the lowest measurable species in dust are IcdP and Bbf with average concentrations of 19 and 27.2 μg kg^{-1}. The total amount of PAHs (ΣPAHs) in Mashhad street dust displayed a very wide range with maximum concentration being 12 times greater than the minimum concentration. ΣPAHs content varies from 764 to 8986.7 μg kg^{-1}, with a mean value of 2183.5 μg kg^{-1}. The highest concentration was observed at Underpass of holy shrine (sample no. S18), with high traffic density (Fig. 3). Limited dispersion of pollutants (Wang et al., 2011) and lack of sunlight (Tobiszewski and Namieśnik, 2012) are probably the main reasons responsible for high concentration of PAHs at this station. These results could be explained by the degenerative photoreactions between PAHs and other pollutants or the volatilization and photo-oxidation of PAHs (especially BaP and BaA) under sunny conditions (Vu et al., 2011). By contrast, the lowest concentration of ΣPAHs was found at Nakhrisi street (sample no. S4), with light traffic load and no industrial plants.

As displayed in Table 10, the PAHs concentration measured in Mashhad street dust samples is higher than those from cities in developing and tropical countries (e.g. Kumasi-Ghana, New Delhi-India, Niteroi-Brazil, Bangalore-India, Hanoi-Vietnam, Lahore-Pakistan, and Greater Cairo-Egypt) but lower than those in China, Japan, UK, and Germany. Also, the average concentrations of total PAHs in Mashhad road dust samples are much higher than those measured in other cities of Iran like Bushehr (1116.2 μg kg^{-1}), Isfahan (1074.6 μg kg^{-1}), and Tehran (330 μg kg^{-1}).

Table 9
Descriptive statistics of PAHs in street dust of Mashhad (μg/kg).

PAHs	Aromatic ring	TEF	Minimum	Maximum	Mean	Median	SD
Naphthalene (Np)	2	0.001	12.00	460.00	96.30	44.00	129.44
Acenaphthene (Ace)	3	0.001	11.00	90.00	30.80	24.00	18.21
Fluorine (Fl)	3	0.001	10.00	80.00	30.20	27.00	18.29
Phenanthrene (Phe)	3	0.001	140.00	1500.00	418.00	380.00	290.79
Anthracene (Ant)	3	0.01	10.00	163.20	36.16	29.00	30.98
Fluoranthene (Flu)	4	0.001	71.00	632.40	370.88	387.60	156.49
Pyrene (Pyr)	4	0.001	140.00	4800.00	598.00	390.00	976.95
Benzo[*a*]anthracene (BaA)	4	0.1	36.00	550.00	150.40	110.00	116.98
Chrysene (Chr)	4	0.01	73.00	540.00	199.25	190.00	103.23
Benzo[*e*]pyrene (BeP)	5	0.01	28.00	130.00	69.30	69.30	25.08
Benzo[*b*]fluoranthene (BbF)	5	0.01	7.20	55.00	27.16	27.16	10.09
Benzo[*k*]fluoranthene (BkF)	5	1	10.00	63.00	36.80	37.00	13.41
Benzo[*a*]pyrene (BaP)	5	1	0.13	70.00	35.06	34.00	16.77
Dibenzo[*ah*]anthracene (DahA)	5	1	8.00	70.00	32.05	32.00	15.86
Benzo[*ghi*]perylene (BghiP)	6	0.01	9.20	78.00	34.11	34.00	17.87
Indene[1,2,3-*cd*]pyrene (IcdP)	6	0.1	4.30	42.00	18.99	18.00	10.79
ΣPAHs			764.00	8986.70	2183.45	1891.20	1736.93
ΣCombPAHs/ΣPAHs			0.58	0.77	0.70	0.71	0.06
LMW			234	2273.2	611.5	526	451.6
HMW			509	6714	1572	1418.8	1304.1
TEQ			62.86	283.63	128.49	121.34	53.02
TEQ/ΣPAHs			0.03	0.11	0.07	0.06	0.02

3.5. Compositional pattern of dust PAHs

The 16 studied PAHs were divided into three groups based on the number of aromatic rings i.e., 2–3 rings, 4 ring, and 5–6 rings PAHs. PAH proportions at all sampling sites varied as follows: 4 rings (45.4–69.6%, mean 57.9%), 2–3 rings (20.5–41.5%, mean 28.5%), and 5–6 rings (5.1–20%, mean 13.4%) (Fig. 4). PAH distribution data for all samples showed minor contributions of low molecular weight PAHs (2–3 rings) such as Np, Ace, and Fl (Fig. 4). This may be due to their increased susceptibility to weathering by oxidation and increased losses due their higher aqueous solubility (Marynowski et al., 2011). Generally speaking, most PAHs found in this study were HMW PAHs (≥4 rings), probably because of the higher persistence of these compounds in urban dust, as well as the tendency of HMW PAHs to accumulate in surface dust that are close to emission sources (Chung et al., 2007). Also, the high fraction of high molecular weight PAHs in total PAHs indicate that they mostly come from petroleum fuels combustion (Liu et al., 2009). The sole exception to this finding is Phe, the most

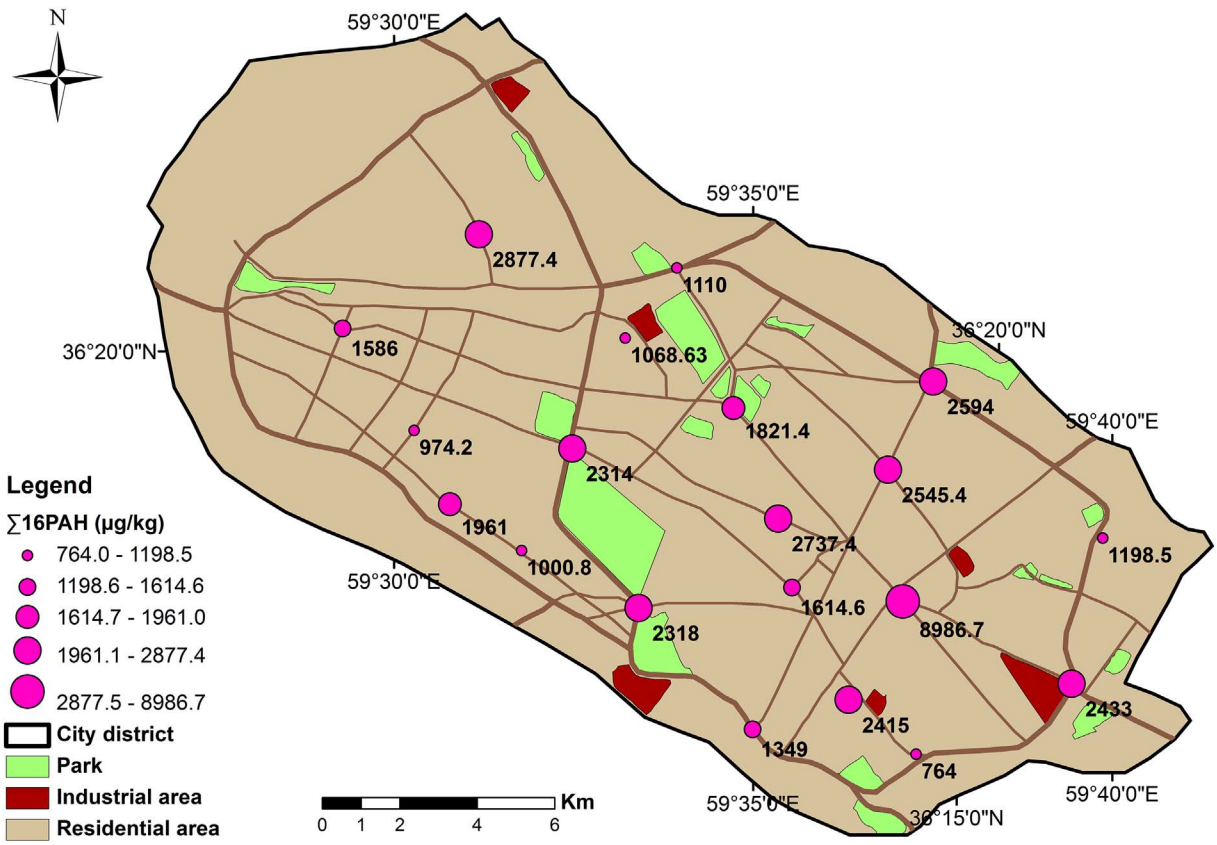

Fig. 3. Map of Σ16 PAHs concentration in the survey area.

Table 10
Comparison of total PAHs in Mashhad street dusts with other cities in the world (Values are in μg kg^{-1}).

City	Number of PAHs	Minimum	Maximum	Mean	Reference
Mashhad (Iran)	16	764	8986.7	2183.5	This study
Bushehr (Iran)	16	73.6	9491	1116.2	Abbasi, 2015
Isfahan (Iran)	16	184.64	3221.72	1074.6	Soltani et al., 2015
Tehran (Iran)	16	130	1410	330	Saeedi et al., 2012
Lanzhou (China)	16	1240	10,700	3900	Jiang et al., 2014
Guangzhou(China)	16	840	12,300	4800	Wang et al., 2009
Kumasi (Ghana)	28	181	7770	1820	Bandowe and Nkansah, 2016
New Delhi (India)	22	650	1700	1100	Tuyen et al., 2014
Niteroi (Brazil)	21	434	1247	–	Pereira Netto et al., 2006
Bangalore (India)	22	670	1800	1100	Tuyen et al., 2014
Hanoi (Vietnam)	22	530	4700	1900	Tuyen et al., 2014
Lahore (Pakistan)	16	120	1000	–	Smith et al., 1995
Tokyo, Japan	34	1400	26,000	–	Takada et al., 1991
Newcastle (UK)	16	590	46,000	–	Lorenzi et al., 2011
Several cities (Germany)	39	3100	21,600	–	Yang and Baumann, 1995
Greater Cairo (Egypt)	16	45	2610	–	Wang et al., 2009

thermodynamically stable of the three-ringed parent PAH, which was also present at relatively high amounts in all Mashhad dust samples (Table 9). As already mentioned, Phe is the second most abundant PAH in Mashhad dust samples. It should be noted that weathering processes such as leaching (solubilization), evaporation/volatilization and biodegradation can modify PAH distribution (Chung et al., 2007). For example, it has been shown that parent PAH and low molecular weight PAHs are more susceptible to microbial degradation than high molecular weight compounds (Douglas et al., 1996).

ΣComb is a sum of Flu, Pyr, BaA, Chr, BkF, BbF, BaP, BghiP, and Ind concentrations, and it represents the typical combustion origin for PAHs (Wang et al., 2009). The ratio of ΣComb/ΣPAHs increases with the fraction of the combustion origin PAHs. The ratio of ΣComb/ΣPAHs in road dust of Mashhad ranged from0.58 to 0.77 with an average of 0.71 (Table 9), representing higher fractions of the combustion origin PAHs.

A complementary approach to characterizing PAHs source (petrogenic vs. pyrogenic) in dust samples is to use PAH isomeric ratios: Anth/(Anth + Phen) and BaA/(BaA + Chrys) compared with Flu/(Flu + Pyr) (Vane et al., 2014) (Fig. 5). In this study, the ratios of Flu/(Flu + Pyr), Ant/(Ant + Phe), BaA/(BaA + Chr) ranged from 0.07 to 0.72, 0.05 to 0.17 and 0.23 to 0.56, respectively. The results indicate that PAHs in the dust samples are mainly derived from petroleum and petroleum combustion products (mixed sources). High traffic load and energy consumption due to urbanization and industrial activity in the study area are the most probable pyrogenic sources of the PAHs.

3.6. Ecotoxicological risk assessment

The cancer potency of each PAH is assessed on the basis of its benzo [*a*]pyrene equivalent concentration (IARC, 2010). Toxic equivalency concentration (TEQ) calculated for street dust of Mashhad metropolis and based on the TEF values is shown in Table 9. TEQ values ranged from 62.9 to 283.6 μg/kg with a mean of 128.5 μg/kg in the study area.

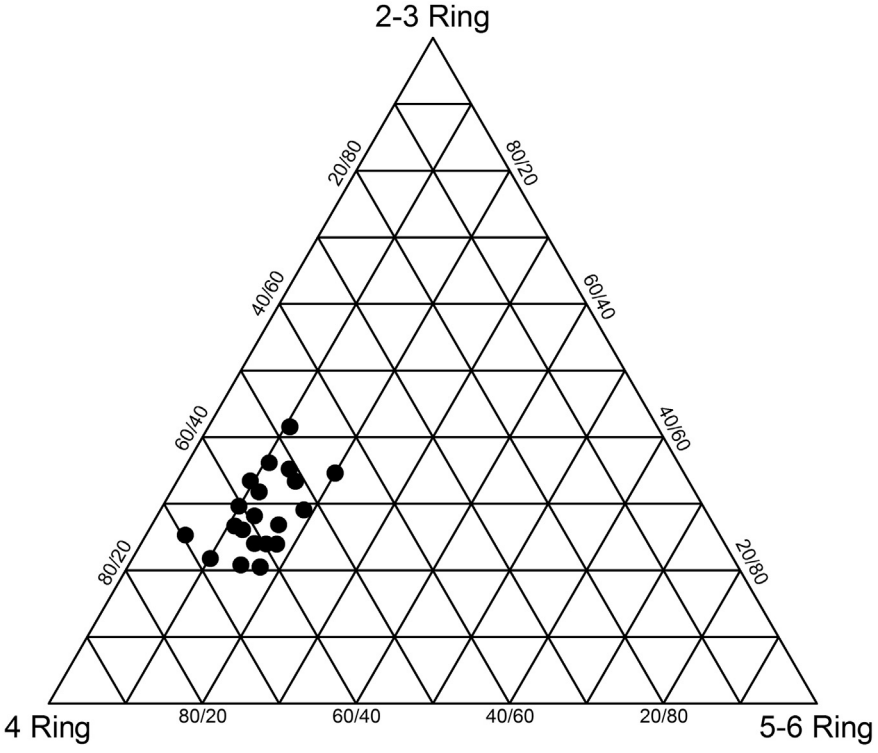

Fig. 4. Triangular diagram of percentage concentration for the PAHs in Mashhad street dust samples.

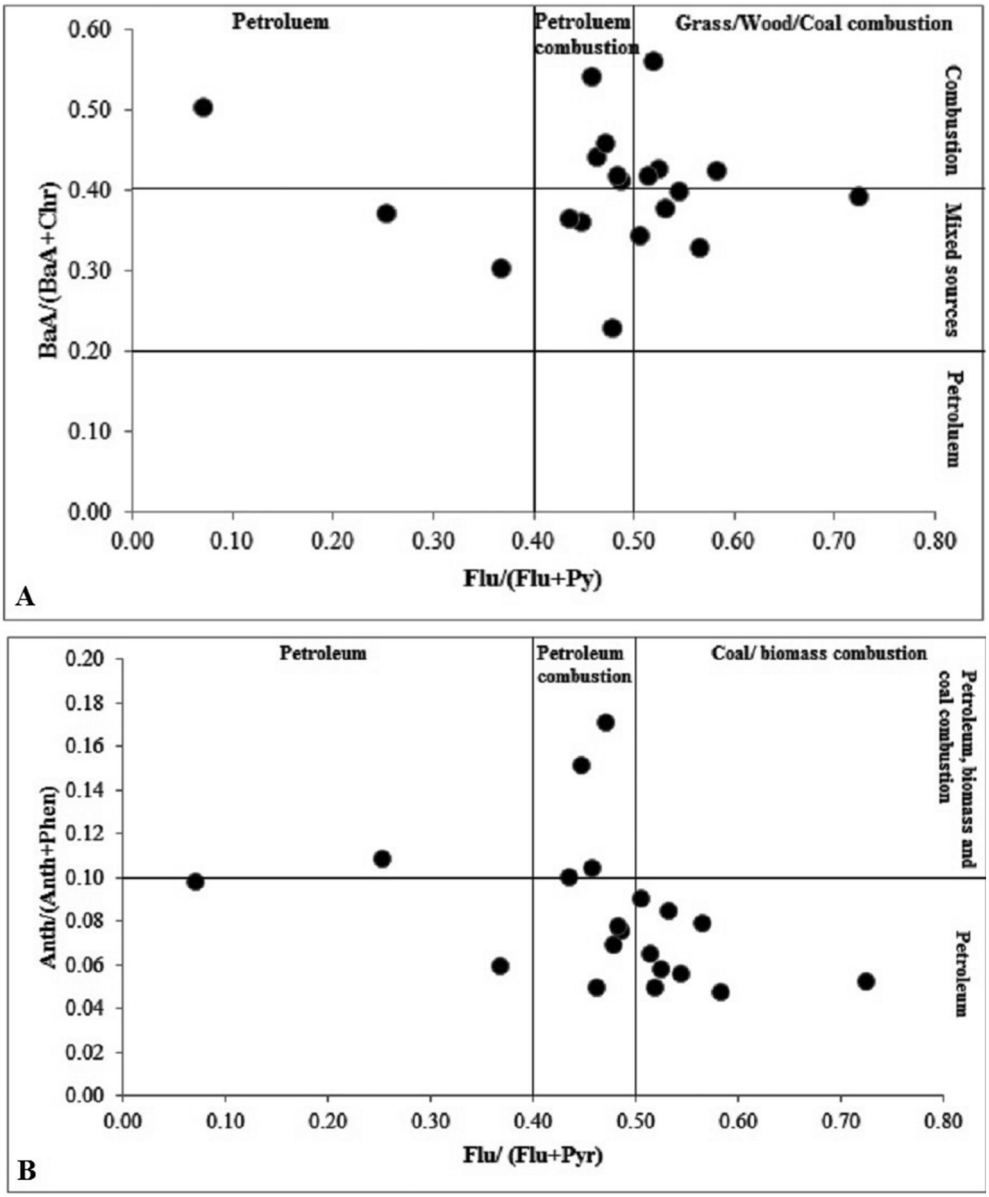

Fig. 5. Plot of the ratios of: (A) BaA/(BaA + Chr) and (B) Anth/(Anth + Phen) vs. Flu/(Flu + Pyr) in Mashhad road dust samples.

High TEQ values were also calculated in samples collected from underpass of the holy shrine (283.6 μg/kg), Azadi square (187.1 μg/kg) and Hor square (179 μg/kg) stations (Fig. 6). In general, the highest TEQ values in street dust samples are measured near sites with heavy traffic load and high overall PAH concentration.

Incremental life cancer risks were employed to investigate the potential cancer risks due to human exposure to environmental PAHs contamination sources (Chen et al., 2013). Carcinogenic potencies relative to TEQ, carcinogenic slope factor (CSF) and probabilistic risk assessment framework were applied to estimate cancer risk incurred from exposure routes to PAHs via inhalation, ingestion and dermal contact (Table 11). The mean cancer risk levels via dermal contact and ingestion pathway are 3.8×10^{-4} and 3.1×10^{-4} in children and 3.9×10^{-4} and 2.2×10^{-4} in adults respectively, which were 10^4 to 10^5 times higher than that via inhalation (6.03×10^{-9} for children and 1.72×10^{-8} for adults) (Table 11). Therefore, the inhalation of resuspended particles through mouth and nose is almost negligible when compared with other pathways. The risk value of direct ingestion for children is slightly higher than the corresponding risk of ingestion for adults. Young children are the most sensitive subpopulation because of their hand-to-mouth activity, whereby contaminated dust can be readily ingested (Meza-Figueroa et al., 2007). In addition, considering the lower body weight of children, the PAHs intake (mg/kg-body-weight/day) of a child is believed to be greater than that of an adult (Wang et al., 2011). Thus, the hazard health risk for children exposed to urban dust PAHs is thought to be greater than that of adults. Compared to children, dermal contact appeared to be the predominant exposure route with relatively higher risk for adults (Table 11). Due to higher dermal exposure area (SA) and exposure duration (ED) values of adults, dermal contact exposure pathway of PAHs had relatively higher risk for adults. This finding was similar to the human cancer risk resulted from PAHs exposure in urban soils of Beijing, China (Peng et al., 2011), and urban surface dust of Guangzhou, China (Wang et al., 2011). The total cancer risk is the sum of risks incurred from exposure routes of ingestion, dermal contact and inhalation. The acceptable risk range for carcinogens is set to 10^{-6}–10^{-4} by the US EPA (2001). Risks below 10^{-6} do not require further action, while risks above 10^{-4} are considered to be of concern and require additional action to reduce the exposure and resulting risk (US EPA, 2001). In the present study, total cancer risk for both children (7×10^{-4}) and adults (6.2×10^{-4}) is

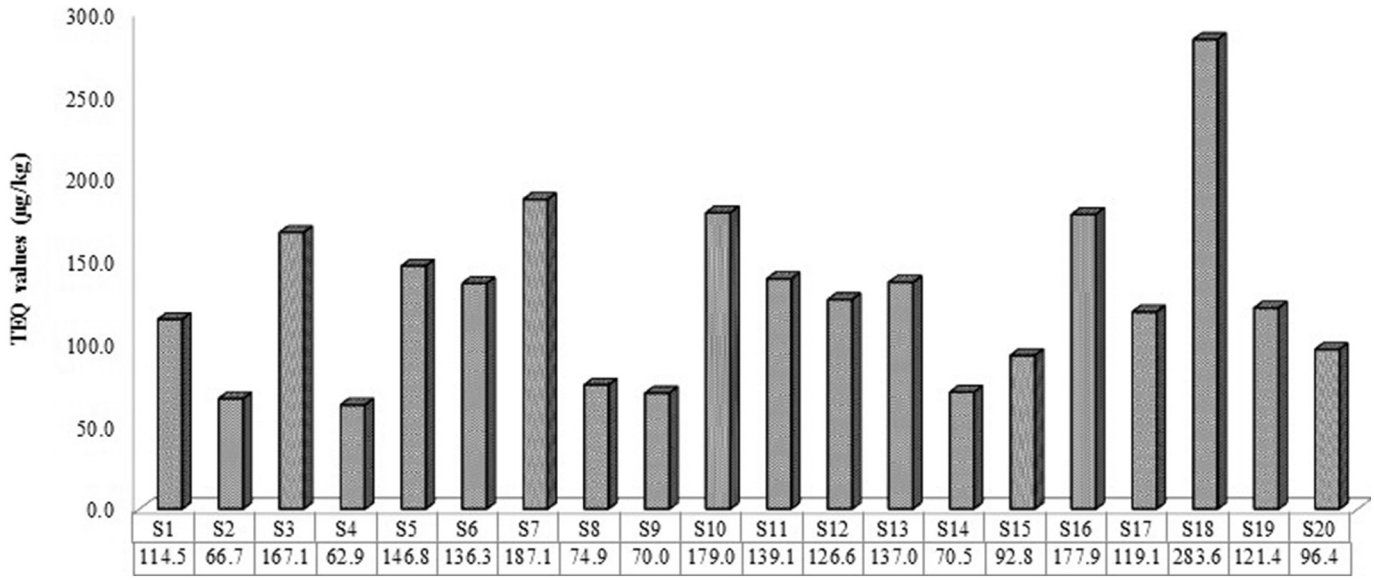

Fig. 6. Calculated TEQ values in the street dust of Mashhad metropolis.

Table 11
The ILCRs for adults and children and cancer risk due to exposure to PAHs in Mashhad metropolis.

Exposure pathways	Child				Adult			
	$ILCRs_{ing}$	$ILCRs_{der}$	$ILCRs_{inh}$	Cancer risk	$ILCRs_{ing}$	$ILCRs_{der}$	$ILCRs_{inh}$	Cancer risk
Mean	0.000311	0.000388	6.03×10^{-9}	0.0007	0.000222	0.000394	1.72×10^{-8}	0.000617
Min	0.000152	0.00019	2.95×10^{-9}	0.000342	0.000109	0.000193	8.44×10^{-9}	0.000302
Max	0.000688	0.000858	1.33×10^{-8}	0.001547	0.000491	0.000872	3.81×10^{-8}	0.001363

higher than the baseline of acceptable risk, indicating a high potential carcinogenic risk. The results suggest that children and adults in Mashhad urban area are exposed to high potential carcinogenic risk via both dust ingestion and dermal contact pathways.

4. Conclusions

The PTEs analysis of street dust samples from different land uses in Mashhad megacity confirmed the clear accumulation of Hg, Cu, Zn, Pb, Sb and Cd. Both the total contents of the studied elements and the oral bioaccessibility estimated by the SBET varied among different land use districts. Distribution of PTEs concentration in the study area indicates that traffic together with the industry are mainly responsible for PTEs pollution, as the highest concentrations and SBET values were found in the high traffic load and industrial areas. The health risk assessment model showed that ingestion of dust particles contributes > 78.0% of the overall non-carcinogenic risk. For both adults and children, Hg and Pb had the highest risk values whereas Cd has the lowest value. The results of this study indicate that PAH concentrations are related to land use, traffic load, emission sources, atmospheric transport, and physiochemical properties of PAH compounds. Source identification based on ring classes and isomeric ratios indicated that there are a variety of PAHs sources in the study area. In this study, total cancer risk for both children (7×10^{-4}) and adults (6.2×10^{-4}) are greater than the recommended level of 10^{-6} and pose a health risk to the residents.

Acknowledgments

The authors wish to express their gratitude to the research committee and medical geology center of Shiraz University (92GRD1M1201) for financial and logistic supports.

References

Abbasi, S., 2015. Geochemistry and Health Hazards of Heavy Metals and Polycyclic Aromatic Hydrocarbons (PAHs) in Road Dusts of Bushehr City. Shiraz University (MSc. Thesis in environmental geology (in Persian)).
Acosta, J.A., Faz, A., Kalbitz, K., Jansen, B., Martinez-Martinez, S., 2011. Heavy metal concentrations in particle size fractions from street dust of Murcia (Spain) as the basis for risk assessment. J. Environ. Monit. 13, 3087–3096.
Adamson, I.Y.R., Prieditis, H., Hedgecock, C., Vincent, R., 2000. Zinc is the toxic factor in the lung response to an atmospheric particulate sample. Toxicol. Appl. Pharmacol. 166, 111–119.
Al-Chalabi, A.S., Hawker, D., 1996. Retention and exchange behavior of vehicular lead in street dusts from major roads. Sci. Total Environ. 187, 105–119.
Al-Khashman, O.A., Shawabkeh, R.A., 2006. Metals distribution in soils around the cement factory in southern Jordan. Environ. Pollut. 140, 387–394.
Amrhein, C., Suarez, D.L., 1987. Calcite super saturation in soils as a result of organic matter mineralization. Soil Sci. Soc. Am. J. 51, 932–937.
Bagherzadeh, A., Mansouri-Daneshvar, M.R., 2011. Physical land suitability evaluation for specific cereal crops using GIS at Mashhad Plain, Northeast of Iran. Front. Agric. China 5 (4), 504–513. http://dx.doi.org/10.1007/s11703-011-1102-6.
Bandowe, B.M., Nkansah, M.A., 2016. Occurrence, distribution and health risk from polycyclic aromatic compounds (PAHs, oxygenated-PAHs and azaarenes) in street dust from a major West African Metropolis. Sci. Total Environ. 553, 439–449. http://dx.doi.org/10.1016/j.scitotenv.2016.02.142.
Boonyatumanond, R., Murakami, M., Wattayakorn, G., Togo, A., Takad, H., 2007. Sources of polycyclic aromatic hydrocarbons (PAHs) in street dust in a tropical Asian megacity, Bangkok, Thailand. Sci. Total Environ. 384, 420–432.
Borji, H., Razmi, Gh., Ahmadi, A., Karami, H., Yaghfoori, S., Abedi, V., 2011. A survey on endoparasites and ectoparasites of stray cats from Mashhad (Iran) and association with risk factors. J. Parasit. Dis. 35 (2), 202–206. http://dx.doi.org/10.1007/s12639-011-0057-0.
Bourliva, A., Papadopoulou, L., Aidona, E., 2016. Study of road dust magnetic phases as the main carrier of potentially harmful trace elements. Sci. Total Environ. 553, 380–391.
Brown, J.N., Peake, B.M., 2006. Sources of heavy metals and polycyclic aromatic hydrocarbons in urban stormwater runoff. Sci. Total Environ. 359, 145–155.
Chen, M., Huang, P., Chen, L., 2013. Polycyclic aromatic hydrocarbons in soils from Urumqi, China: distribution, source contributions, and potential health risks. Environ. Monit. Assess. 185, 5639–5651.
Chung, M.K., Hu, R., Cheng, K.C., Wong, M.H., 2007. Pollutants in Hong Kong soils: polycyclic aromatic hydrocarbons. Chemosphere 67, 464–473.
De Miguel, E., Llamas, J.F., Chacón, E., Berg, T., Larssen, S., Røyset, O., Vadset, M., 1997.

Origin and patterns of distribution of trace elements in street dust: unleaded petrol and urban lead. Atmos. Environ. 31, 2733–2740.
Douglas, G.S., Bence, A.E., Prince, R.C., McMillen, S.J., Butler, E.L., 1996. Environmental stability of selected petroleum hydrocarbon source and weathering ratio. Environ. Sci. Technol. 38, 3958–3964.
Emamapour, S.R., Borji, H., Nagibi, A., 2015. An epidemiological survey on intestinal helminths of stray dogs in Mashhad, North-east of Iran. J. Parasit. Dis. 39 (2), 266–271. http://dx.doi.org/10.1007/s12639-013-0319-0.
Fang, F.M., Wang, H.D., Lin, Y.S., 2011. Spatial distribution, bioavailability, and health risk assessment of soil Hg in Wuhu urban area, China. Environ. Monit. Assess. 179, 255–265.
Fergusson, J.E., Ryan, D.E., 1984. The elemental composition of street dust from large and small urban areas related to city type, source and particle-size. Sci. Total Environ. 34, 101–116.
Ferreira-Baptista, L., De Miguel, E., 2005. Geochemistry and risk assessment of street dust in Luanda, Angola: a tropical urban environment. Atmos. Environ. 39, 4501–4512.
Gee, G.W., Bauder, J.W., 1986. Particle-size analysis. In: Klute, A. (Ed.), Methods of Soil Analysis. Part 1. Physical and Mineralogical Methods, 2nd ed. Agronomy Monograph No. 9 American Society of Agronomy/Soil Science Society of America, Madison, pp. 383–411.
Ghazi, A., Hafezi-Moghadas, N., Sadeghi, H., Ghafoori, M., Lashkaripour, Gh.R., 2015. Dynamic soil properties of some deep trenches in Mashhad city, NE Iran. J. Earth Syst. Sci. 124 (7), 1417–1428.
Granero, S., Domingo, J., 2002. Levels of metals in soils of Alcalá de Henares, Spain: human health risks. Environ. Int. 28, 159–164.
Heiri, O., Lotter, A.F., Lemcke, G., 2001. Loss on ignition as a method for estimating organic and carbonate content in sediments: reproducibility and comparability of results. J. Paleolimnol. 25 (1), 101–110.
Hu, X., Zhang, Y., Luo, J., Wang, T.J., Lian, H.Z., Ding, Z.H., 2011. Bioaccessibility and health risk of arsenic, mercury and other metals in urban street dusts from a mega-city, Nanjing, China. Environ. Pollut. 159, 1215–1221.
Hwang, H.M., Wade, T.L., Sericano, J.L., 2003. Concentrations and source characterization of polyaromatic hydrocarbons in pine needles from Korea, Mexico, and United States. Atmos. Environ. 37, 2259–2267.
International Agency for Research on Cancer (IARC), 2010. Some non-heterocyclic polycyclic aromatic hydrocarbons and some related exposures. In: IARC Monographs on the Evaluation of Carcinogenic Risks to Humans. 92 (Lyon France).
Jiang, Y.F., Hu, X.F., Yves, U.J., Zhan, H.Y., Wu, Y.Q., 2014. Status, source and health risk assessment of polycyclic aromatic hydrocarbons in street dust of an industrial city, NW China. Ecotoxicol. Environ. Saf. 106, 11–18.
Jiries, A.G., Hussein, H.H., Halash, Z., 2001. The quality of water and sediments of street runoff in Amman, Jordan. Hydrol. Process. 15, 815–824.
Karimi, A., Haghnia, G.H., Safari, T., Hadadian, H., 2017. Lithogenic and anthropogenic pollution assessment of Ni, Zn and Pb in surface soils of Mashhad plain, northeastern Iran. Catena 157, 151–162. http://dx.doi.org/10.1016/j.catena.2017.05.019.
Karmacharya, N., Shakya, P.R., 2012. Heavy metals in bulk and particle size fractions from street dust of Kathmandu as the possible basis for risk assessment. Sci. World J. 10 (10), 84–88.
Keshavarzi, B., Tazarvi, Z., Rajabzadeh, M.A., Najmeddin, A., 2015. Chemical speciation, human health risk assessment and pollution level of selected heavy metals in urban street dust of Shiraz, Iran. Atmos. Environ. 119, 1–10.
Keshavarzi, B., Abbasi, S., Moore, F., Delshab, H., Soltani, N., 2017. Polycyclic aromatic hydrocarbons in street dust of Bushehr City, Iran: status, source, and human health risk assessment. Polycycl. Aromat. Compd. http://dx.doi.org/10.1080/10406638.2017.1354897.
Klees, M., Hiester, E., Bruckmann, P., Schmidt, T., 2013. Determination of polychlorinated biphenyls and polychlorinated dibenzo-*p*-dioxins and dibenzofurans by pressurized liquid extraction and gas chromatography coupled to mass spectrometry in street dust samples. J. Chromatogr. A 1300, 17–23.
Krishna, A.K., Mohan, K.R., 2013. Metal contamination and their distribution in different grain size fractions of sediments in an industrial development area. Bull. Environ. Contam. Toxicol. 90, 170–175.
Kumar, V., Kothiyal, N.C., 2011. Distribution behavior of polycyclic aromatic hydrocarbons in roadside soil at traffic intercepts within developing cities. Int. J. Environ. Sci. Technol. 8, 63–72.
Lee, B., Dong, T., 2010. Effects of road characteristics on distribution and toxicity of polycyclic aromatic hydrocarbons in urban road dust of Ulsan, Korea. J. Hazard. Mater. 175, 540–550.
Li, J., Huang, Y., Ye, R., Yuan, G.L., Wu, H.Z., Han, P., Fu, Sh., 2015. Source identification and health risk assessment of Persistent Organic Pollutants (POPs) in the topsoils of typical petrochemical industrial area in Beijing, China. J. Geochem. Explor. 158, 177–185. http://dx.doi.org/10.1016/j.gexplo.2015.07.014.
Liu, Y., Chen, L., Huang, Q., Li, W.Y., Tang, Y.J., Zhao, J.F., 2009. Source apportionment of polycyclic aromatic hydrocarbons (PAHs) in surface sediments of the Huangpu River, Shanghai, China. Sci. Total Environ. 407, 2931–2938.
Liu, E., Yan, T., Birch, G., Zhu, Y., 2014. Pollution and health risk of potentially toxic metals in urban road dust in Nanjing, a mega-city of China. Sci. Total Environ. 476, 522–531.
Lorenzi, D., Entwistle, J.A., Cave, M., Dean, J.R., 2011. Determination of polycyclic aromatic hydrocarbons in urban street dust: implications for human health. Chemosphere 83, 970–977.
Lu, X., Wang, L., Li, L.Y., Lei, K., Huang, L., Kang, D., 2010. Multivariate statistical analysis of heavy metals in street dust of Baoji, NW China. J. Hazard. Mater. 173, 744–749. http://dx.doi.org/10.1016/j.jhazmat.2009.09.001.
Lu, Y., Jia, C., Zhang, G., Zhao, Y., Wilson, M.A., 2016. Spatial distribution and source of potential toxic elements (PTEs) in urban soils of Guangzhou, China. Environ. Earth Sci. 75, 329. http://dx.doi.org/10.1007/s12665-015-5190-0.
Luo, X., Yu, S., Zhu, Y., Li, X., 2012. Trace metal contamination in urban soils of China. Sci. Total Environ. 421–422, 17–30.
Malkoc, S., Yazici, B., Koparal, S., 2010. Assessment of the levels of heavy metal pollution in roadside soils of Eskisehir, Turkey. Environ. Toxicol. Chem. 29 (12), 2720–2725.
Marynowski, L., Kurkiewicz, S., Rakocin'ski, M., Simoneit, B.R.T., 2011. Effects of weathering on organic matter: I. Changes in molecular composition of extractable organic compounds caused by paleoweathering of a Lower Carboniferous (Tournaisian) marine black shale. Chem. Geol. 285, 144–156.
Mashal, Kh., Salahat, M., Al-Qinna, M., Al-Degs, Y., 2015. Spatial distribution of cadmium concentrations in street dust in an arid environment. Arab. J. Geosci. 8, 3171–3182. http://dx.doi.org/10.1007/s12517-014-1367-1.
Metson, A.J., 1961. Methods of Chemical Analysis of Soil Survey Samples. Govt. Printers, Wellington, New Zealand.
Meza-Figueroa, D., O-Villanueva, M., Parra, M.L., 2007. Heavy metal distribution in dust from elementary schools in Hermosillo, Sonora, México. Atmos. Environ. 41, 276–288.
Mohd Han, N.M., Latif, M.T., Othman, M., Dominick, D., Mohamad, N., Juahir, H., Tahir, N.M., 2014. Composition of selected heavy metals in road dust from Kuala Lumpur city centre. Environ. Earth Sci. 72, 849–859. http://dx.doi.org/10.1007/s12665-013-3008-5.
Muller, G., 1981. Die Schwermetallbelstang der sediment des Neckarars und seiner N ebenflusseeine estandsauf nahme. Chemical Zeitung 105, 157–164.
Najmeddin, A., Keshavarzi, B., Moore, F., Lahijanzadeh, A., 2017. Source apportionment and health risk assessment of potentially toxic elements in road dust from urban industrial areas of Ahvaz megacity, Iran. Environ. Geochem. Health. http://dx.doi.org/10.1007/s10653-017-0035-2.
Nazzal, Y., Ghrefat, H., Rosen, M., 2014. Application of multivariate geostatistics in the investigation of heavy metal contamination of roadside dusts from selected highways of the Greater Toronto Area, Canada. Environ. Earth Sci. 71, 1409–1419. http://dx.doi.org/10.1007/s12665-013-2546-1.
Net, S., El-Osmani, R., Prygiel, E., Rabodonirina, S., Dumoulin, D., Ouddane, B., 2015. Overview of persistent organic pollution (PAHs, Me-PAHs and PCBs) in freshwater sediments from Northern France. J. Geochem. Explor. 148, 181–188. http://dx.doi.org/10.1016/j.gexplo.2014.09.008.
Nisbet, C., LaGoy, P., 1992. Toxic equivalency factors (TEFs) for polycyclic aromatic hydrocarbons (PAHs). Regul. Toxicol. Pharmacol. 16, 290–300.
Okorie, A., Entwistle, J., Dean, J.R., 2012. Estimation of daily intake of potentially toxic elements from urban street dust, and the role of oral bioaccessibility testing. Chemosphere 86, 460–467.
Peng, C., Chen, W.P., Liao, X.L., Wang, M.E., Ouyang, Z.Y., Jiao, W.T., et al., 2011. Polycyclic aromatic hydrocarbons in urban soils of Beijing: status, sources, distribution and potential risk. Environ. Pollut. 159, 802–808.
Pereira Netto, A.D., Krauss, T., Cunha, I., Rego, E., 2006. PAHs in SD: polycyclic aromatic hydrocarbons levels in street dust in the central area of Niterói City, RJ, Brazil. Water Air Soil Pollut. 176, 57–67.
Qi, L., Gregoire, D.C., 2000. Determination of trace elements in twenty-six Chinese geochemistry reference materials by inductively coupled plasma-mass spectrometry. Geostand. Geoanal. Res. 24, 51–63.
Ravankhah, N., Mirzaei, R., Masoumi, S., 2017. Determination of heavy metals in surface soils around the brick kilns in an arid region, Iran. J. Geochem. Explor. 176, 91–99.
Ray, S., Khillare, P.S., Agarwal, T., Shridhar, V., 2008. Assessment of PAHs in soil around the International Airport in Delhi, India. J. Hazard. Mater. 156, 9–16.
Rudnick, R.L., Gao, S., 2003. Composition of the continental crust. In: Rudnick, R.L. (Ed.), The Crust. Elsevier.
Ryan, J., Estefan, G., Rashid, A., 2007. Soil and Plant Analysis Laboratory Manual. ICARDA, Aleppo, Syria.
Saeedi, M., Li, L.Y., Salmanzadeh, M., 2012. Heavy metals and polycyclic aromatic hydrocarbons: pollution and ecological risk assessment in street dust of Tehran. J. Hazard. Mater. 227-228, 9–17.
Salmanzadeh, M., Saeedi, M., Li, L.Y., Nabi-Bidhendi, Gh., 2015. Characterization and metals fractionation of street dust samples from Tehran, Iran. Int. J. Environ. Res. 9 (1), 213–224.
Schafer, J., Norra, S., Klein, D., Blanc, G., 2009. Mobility of trace metals associated with urban particles exposed to natural waters of various salinities from the Gironde Estuary, France. J. Soils Sediments 9, 374–392.
Sezgin, N., Kurtulus, H., Demir, G., Nemlioglu, S., Bayat, C., 2004. Determination of heavy metal concentration in street dusts in Istanbul E-5 highway. Environ. Int. 29, 979–985.
SGS, 2014. Analytical services. www.sgs.com/geochem.
Shaddel, M., Shokouhian, M., 2014. Feasibility of solar thermal collectors usage in dwelling apartments in Mashhad, the second megacity of Iran. Renew. Sust. Energ. Rev. 39, 1200–1207.
Shepard, F.P., 1954. Nomenclature based on sandsiltclay ratios. J. Sediment. Petrol. 24, 151–158.
Sialelli, J., Urquhart, G.J., Davidson, C.M., Hursthouse, A.S., 2010. Use of a physiologically based extraction test to estimate the human bioaccessibility of potentially toxic elements in urban soils from the city of Glasgow, UK. Environ. Geochem. Health 32 (6), 517–527. http://dx.doi.org/10.1007/s10653-010-9314-x.
Smith, D.J.T., Edelhauser, E.C., Harrison, R.M., 1995. Polynuclear aromatic hydrocarbon concentrations in road dust and soil samples collected in the United Kingdom and Pakistan. Environ. Technol. 16, 45–53.
Soltani, N., Keshavarzi, B., Moore, F., Tavakol, T., Lahijanzadeh, A.R., Jaafarzadeh, N., Kermani, M., 2015. Ecological and human health hazards of heavy metals and polycyclic aromatic hydrocarbons (PAHs) in road dust of Isfahan metropolis, Iran. Sci. Total Environ. 505, 712–723.

Sun, G., Li, Z., Bi, X., Chen, Y., Lu, S., Yuan, X., 2013. Distribution, sources and health risk assessment of mercury in kindergarten dust. Atmos. Environ. 73, 169–176.
Takada, H., Onda, T., Harada, M., Ogura, N., 1991. Distribution and sources of polycyclic aromatic hydrocarbons (PAHs) in street dust from the Tokyo Metropolitan area. Sci. Total Environ. 107, 45–69.
Tang, R., Ma, K., Zhang, Y., Mao, Q., 2013. The spatial characteristics and pollution levels of metals in urban street dust of Beijing, China. Appl. Geochem. 35, 88–98.
Tobiszewski, M., Namieśnik, J., 2012. PAH diagnostic ratios for the identification of pollution emission sources. Environ. Pollut. 162, 110–119.
Trujillo-González, J.M., Torres-Mora, M.A., Keesstra, S., Brevik, E., Jiménez-Ballesta, R., 2016. Heavy metal accumulation related to population density in road dust samples taken from urban sites under different land uses. Sci. Total Environ. 553, 636–642.
Tumuklu, A., Yalcin, M.G., Sonmez, M., 2007. Detection of heavy metal concentrations in soil caused by Nigde City Garbage Dump. Pol. J. Environ. Stud. 16, 651–658.
Tuyen, L.H., Tue, N.M., Takahashi, S., Suzuki, G., Viet, P.H., Subramanian, A., Bulbule, K.A., Parthasarathy, P., Ramanathan, A., Tanabe, S., 2014. Methylated and unsubstituted polycyclic aromatic hydrocarbons in street dust from Vietnam and India: occurrence, distribution and in vitro toxicity evaluation. Environ. Pollut. 194, 272–280.
U.S. Environmental Protection Agency (EPA), 1996. Soil screening guidance: technical background document. In: Office of Solid Waste and Emergency Response (EPA/540/R-95/128).
U.S. Environmental Protection Agency (EPA), 2001. Supplemental guidance for developing soil screening levels for superfund sites. In: Office of Solid Waste and Emergency Response 9355. OSWER, pp. 20014–20024.
U.S. Environmental Protection Agency (EPA), 2008. Standard Operating Procedure for an In Vitro Bioaccessibility Assay for Lead in Soil EPA 9200. pp. 1–86.
Valdez Cerda, E., Reyes, L.H., Alfaro Barbosa, J.M., Elizondo-Martinez, P., Acuña-Askar, K., 2011. Contamination and chemical fractionation of heavy metals in street dust from the Metropolitan Area of Monterrey, Mexico. Environ. Technol. 32 (10), 1163–1172. http://dx.doi.org/10.1080/09593330.2010.529466.
Vane, C.H., Kim, A.W., Beriro, D.J., Cave, M.R., Knights, K., Moss-Hayes, V., Nathanail, P.C., 2014. Polycyclic aromatic hydrocarbons (PAH) and polychlorinated biphenyls (PCB) in urban soils of Greater London, UK. Appl. Geochem. 51, 303–314.
Vu, V.T., Lee, B.K., Kim, J.T., Lee, C.H., Kim, I.H., 2011. Assessment of carcinogenic risk due to inhalation of polycyclic aromatic hydrocarbons in PM_{10} from an industrial city: a Korean case study. J. Hazard. Mater. 189, 349–356.
Wang, X.S., Qin, Y., Chen, Y.K., 2007. Leaching characteristics of arsenic and heavy metals in urban roadside soils using a simple bioavailability extraction test. Environ. Monit. Assess. 129, 221–226.
Wang, D.G., Yang, M., Jia, H.L., Zhou, L., Li, Y.F., 2009. Polycyclic aromatic hydrocarbons in urban street dust and surface soil: comparisons of concentration, profile, and source. Arch. Environ. Contam. Toxicol. 56, 173–180.
Wang, W., Huang, M.J., Kang, Y., Wang, H.S., Leung, A.O.W., Cheung, K.C., Wong, M.H., 2011. Polycyclic aromatic hydrocarbons (PAHs) in urban surface dust of Guangzhou, China: status, sources and human health risk assessment. Sci. Total Environ. 409, 4519–4527.
Webster, R., Oliver, M.A., 2001. Geostatistics for Environmental Scientists. John Wiley & Sons Ltd, Chichester.
Wei, B., Jiang, F., Li, X., Mu, S., 2010. Contamination levels assessment of potential toxic metals in road dust deposited in different types of urban environment. Environ. Earth Sci. 61, 1187–1196. http://dx.doi.org/10.1007/s12665-009-0441-6.
Yang, Y., Baumann, W., 1995. Seasonal and areal variations of polycyclic aromatic hydrocarbon concentrations in street dust determined by super critical fluid extraction and gas chromatography–mass spectrometry. Analyst 120, 243–248.
Yildırım, G., Tokalıoğlu, S., 2016. Heavy metal speciation in various grain sizes of industrially contaminated street dust using multivariate statistical analysis. Ecotoxicol. Environ. Saf. 124, 369–376.
Zannoni, D., Valotto, G., Visin, F., Rampazzo, G., 2016. Sources and distribution of tracer elements in road dust: the Venice mainland case of study. J. Geochem. Explor. 166, 64–72. http://dx.doi.org/10.1016/j.gexplo.2016.04.007.
Zhang, C., McGrath, D., 2004. Geostatistical and GIS analyses on soil organic carbon concentrations in grassland of southeastern Ireland from two different periods. Geoderma 119, 261–275.
Zhang, C., Qiao, Q., Appel, E., Huang, B., 2012. Discriminating sources of anthropogenic heavy metals in urban street dusts using magnetic and chemical methods. J. Geochem. Explor. 119–120, 60–75.
Zhao, N., Lu, X., Chao, Sh., 2016. Risk assessment of potentially toxic elements in smaller than 100-μm street dust particles from a valley-city in northwestern China. Environ. Geochem. Health 38, 483–496. http://dx.doi.org/10.1007/s10653-015-9734-8.
Zheng, N., Liu, J., Wang, Q., Liang, Z., 2010. Health risk assessment of heavy metal exposure to street dust in the zinc smelting district, Northeast of China. Sci. Total Environ. 408, 726–733.
Žibret, G., 2012. Impact of dust filter installation in ironworks and construction on brownfield area on the toxic metal concentration in street and house dust (Celje, Slovenia). Ambio 41 (3), 292–301. http://dx.doi.org/10.1007/s13280-011-0188-7.
Žibret, G., 2013. Organic compounds in the urban dusts in Celje area. Geologia 56 (1), 87–96. http://dx.doi.org/10.5474/geologija.2013.007.
Žibret, G., Van Tonder, D., Žibret, L., 2013. Metal content in street dust as a reflection of atmospheric dust emissions from coal power plants, metal smelters, and traffic. Environ. Sci. Pollut. Res. 20 (7), 4455–4468. http://dx.doi.org/10.1007/s11356-012-1398-7.